Petroleum Science 22 (2025) 1625–1652

Contents lists available at ScienceDirect

Petroleum Science

journal homepage: www.keaipublishing.com/en/journals/petroleum-science

Review Paper

Fracture propagation mechanism and application of supercritical CO_2 fracturing in shale: A review

Yuan-Xiu Sun [a], Xiao-Long Wang [a,*], Yan-Zhao Meng [b], Jin-Long Tian [b], Cheng-Hui Lu [b]

[a] College of Petroleum Engineering, Liaoning Petrochemical University, Fushun, 113001, Liaoning, China
[b] Baikouquan Oil Production Plant of Petrochina Xinjiang Oilfield Branch, Karamay, 834000, Xinjiang, China

ARTICLE INFO

Article history:
Received 27 May 2024
Received in revised form
23 November 2024
Accepted 23 January 2025
Available online 29 January 2025

Edited by Min Li

Keywords:
Supercritical CO_2
Waterless fracturing
Shale oil and gas reservoirs
Fracture formation mechanism
Fracturing technology

ABSTRACT

With the increasing demand for energy, traditional oil resources are facing depletion and insufficient supply. Many countries are rapidly turning to the development of unconventional oil and gas resources. Among them, shale oil and gas reservoirs have become the focus of unconventional oil and gas resources exploration and development. Based on the characteristics of shale oil and gas reservoirs, supercritical CO_2 fracturing is more conducive to improving oil recovery than other fracturing technologies. In this paper, the mechanism of fracture initiation and propagation of supercritical CO_2 in shale is analyzed, including viscosity effect, surface tension effect, permeation diffusion effect of supercritical CO_2, and dissolution-adsorption effect between CO_2 and shale. The effects of natural factors, such as shale properties, bedding plane and natural fractures, and controllable factors, proppant, temperature, pressure, CO_2 concentration and injection rate on fracture initiation and propagation are clarified. The methods of supercritical CO_2 fracturing process, thickener and proppant optimization to improve the efficiency of supercritical CO_2 fracturing are discussed. In addition, some new technologies of supercritical CO_2 fracturing are introduced. The challenges and prospects in the current research are also summarized. For example, supercritical CO_2 is prone to filtration when passing through porous media, and it is difficult to form a stable flow state. Therefore, in order to achieve stable fracturing fluid suspension and effectively support fractures, it is urgent to explore new fracturing fluid additives or improve fracturing fluid formulations combined with the research of new proppants. This paper is of great significance for understanding the behavior mechanism of supercritical CO_2 in shale and optimizing fracturing technology.

1. Introduction

With the growth of global population and the development of economy, the demand for energy is increasing. Due to the gradual depletion and insufficient supply of traditional oil resources, many countries have begun to seek to develop unconventional oil and gas reservoirs to fill the energy gap. Shale oil and gas reservoir is an important part of unconventional oil and gas reservoirs, and it is also a hot spot in the exploration and development of unconventional oil and gas resources (Kang, 2012; Kang and Zhou, 2016). Based on the characteristics of shale oil and gas reservoirs, it is difficult to effectively exploit shale oil and gas resources through natural production capacity. Fracturing technology is the main means of increasing production of shale oil and gas (Bhandari et al., 2015; Heller et al., 2014; Liao, 2021). Hydraulic fracturing is the most conventional fracturing technology, which has been widely used in the process of commercial development of unconventional oil and gas such as shale gas (Denneyd, 2010). However, large-scale hydraulic fracturing faces a series of challenges such as waste of water, back flow water pollution (Scanlon et al., 2014; M. Wang et al., 2018), pore blockage and formation damage (Bahrami et al., 2012; Bazin et al., 2010; Kargbo et al., 2010). In order to reduce consumption of water resources and environmental risks in the process of unconventional reservoir reconstruction, waterless fracturing technologies such as supercritical CO_2($SC\text{-}CO_2$) have attracted more and more attention (Liu et al., 2017; Xian et al., 2015; J.P. Zhou et al., 2022). At present, waterless fracturing technologies mainly include liquid CO_2 fracturing, liquid N_2 fracturing, liquefied

* Corresponding author.
E-mail address: wxl184389@163.com (X.-L. Wang).

https://doi.org/10.1016/j.petsci.2025.01.009
1995-8226/

petroleum gas fracturing, self-supporting fracturing and SC-CO_2 fracturing. When the pressure of liquid CO_2 fracturing decreases, CO_2 may freeze under reservoir conditions and form hydrates to plug the wellbore (Li et al., 2024; Wang et al., 2014). During liquid N_2 fracturing, when N_2 enters the formation, the proppant transport capacity will be reduced. In addition, the equipments for treating liquid N_2 are limited (Cai et al., 2014; Huang et al., 2020). Liquefied petroleum gas fracturing has high cost, belonging to high-risk gas, which has strong flammability and safety problems (J.Z. Zhao et al., 2018). The phase state of the self-supporting fracturing fluid cannot be ideally transformed, and the leaking fracturing fluid may cause the matrix pores to be blocked (Luo et al., 2020; Zhang et al., 2022). The SC-CO_2, as a fracturing fluid, possessing unique physical and chemical properties, can effectively avoid the above problems. It can be fully applied in shale oil and gas reservoirs, and replace methane in shale matrix, which helps to improve natural gas recovery and CO_2 storage (Khosrokhavar et al., 2014; J.P Zhou et al., 2019).

SC-CO_2 fracturing technology is regarded as a waterless fracturing method with great potential. When the temperature exceeds 31.1 °C and the pressure exceeds 7.38 MPa, CO_2 is converted to a supercritical state. SC-CO_2 is between liquid and gas, with density close to that of liquid, viscosity coefficient close to that of gas. SC-CO_2 has extremely low surface tension, high diffusion coefficient and strong penetration capacity. Minerals in shale can be dissolved due to characteristics, which can improve permeability, resulting in more pores and fractures (Akono et al., 2019; Gutierrez et al., 2015). SC-CO_2 has low viscosity and high penetration capacity, which makes it have good fluidity and diffusivity in the process of mass transfer and heat transfer. Hence, SC-CO_2 can penetrate into the tiny pores and fractures in shale, which form a complex fracture network (Hashemi and Zoback, 2021; Sun et al., 2019). SC-CO_2 will expand in rock under high pressure and high temperature, thus increasing the internal stress of rock. This expansion can lead to stress failure of rock, form fractures and promote the expansion of fractures (Lu et al., 2018). During fracturing, there is no water in the fluid, which will not cause the expansion of the reservoir clay and increase the fracturing effect, thereby improving the exploitation efficiency of shale oil and gas (G.S. Li et al., 2013; Wang et al., 2012; H.Z. Wang et al., 2019). Therefore, SC-CO_2 fracturing technology has broad application prospects in the study of improving the fracturing efficiency of shale reservoirs.

With the commercialization of unconventional oil and gas, researchers have begun to have an in-depth understanding of SC-CO_2 fracturing technology. It is of great significance to explore the fracture initiation and propagation of shale reservoirs to improve oil recovery. According to the thermophysical properties and shale reservoir properties of SC-CO_2, Wang et al. (2012) conducted a comprehensive feasibility study on the application potential of SC-CO_2 in shale reservoirs, which proved that SC-CO_2 has great potential for exploiting shale oil and gas reservoir resources. Yin et al. (2017) found that the effect of CO_2 will weaken the uniaxial compressive strength and elastic modulus of shale. The weakening effect of SC-CO_2 is more significant than that of gaseous CO_2, indicating that the crack propagation ability is related to the elastic modulus of shale. Based on the research of Yin et al. (2017), Lyu et al. (2018) found that with the increase of SC-CO_2 injection pressure, the compressive strength and elastic modulus of shale gradually decreased. Tian et al. (2023) also further studied the effect of SC-CO_2 on weakening the tensile strength of shale, and the weakening degree gradually increased with the increase of action time. Due to the unique physical and chemical properties of SC-CO_2, it has great advantages in the process of rock fracture initiation. Ishida et al. (2012) studied the characteristics of fracture initiation pressure of SC-CO_2 on rocks through experiments, and compared it with liquid CO_2 fracturing. The results showed that the initiation pressure of SC-CO_2 fracturing is lower than that of liquid CO_2 fracturing. Lu et al. (2018) compared SC-CO_2 fracturing with hydraulic fracturing by performing true triaxial tests on shale outcrops and sandstones. The results showed that the initiation pressure of SC-CO_2 fracturing is about 50.9% lower than that of hydraulic fracturing in shale. For fracture morphology, Y.Q. Chen et al. (2015) and Kizaki et al. (2013) compared the fracture propagation modes of SC-CO_2, water and heavy oil during fracturing. The results demonstrated that SC-CO_2 fracturing fractures show more branches, and the fracture morphology tends to be more complex. Su et al. (2019) studied that SC-CO_2 has good diffusivity and permeability through simulation experiments, which can penetrate into the surrounding rock and increase pore pressure, thus reducing the limitation of in-situ stress on fracture propagation. Although researchers have conducted a large number of fracturing experiments, SC-CO_2 fracturing is greatly affected by rock properties, underground conditions, fracturing equipment and other factors. Therefore, we must fully consider its fracture initiation and propagation under real reservoir conditions, and make sure the influence of controllable factors on the fracturing effect. This will help us better understand its behavior in underground reservoirs and provide guidance for practical applications. In addition, we also need to consider the long-term impact of SC-CO_2 fracturing on reservoir rocks to ensure reservoir stability and sustainability of energy development after fracturing.

In this paper, the mechanism of SC-CO_2 initiation and fracture propagation in shale is described. Through the analysis of experimental research, the influence of various factors on shale initiation and fracture propagation in the fracturing process is considered. The method of improving the efficiency of SC-CO_2 fracturing is discussed. Other SC-CO_2 fracturing technologies for shale reservoirs are summarized, and the application of new technologies is also discussed. Finally, the problems existing in the current research and the possibility of new technologies for shale reservoirs are analyzed, and suggestions for future research are put forward.

2. Study on fracture initiation and propagation of supercritical CO_2 in shale

2.1. Fracture initiation and propagation mechanism

When CO_2 enters the shale reservoir to reach a critical state, SC-CO_2 fractures the shale through its own unique physical properties, such as viscosity similar to gas, extremely low surface tension, etc. Furthermore, the penetration ability of SC-CO_2 and the interaction with shale can expand the porosity and permeability of shale, and reduce the compressive strength and elastic modulus of shale. This will accelerate the occurrence of fracture initiation mechanism.

2.1.1. Low viscosity effect of supercritical CO_2

SC-CO_2 has lower viscosity, so it has better fluidity. The permeability of shale can be improved after fracturing treatment. When SC-CO_2 enters shale, it can more easily penetrate into the tiny pores and fractures of the rock, promoting fracture expansion. At the same time, this low viscosity can reduce energy consumption and improve injection efficiency, making it flow more smoothly in rock pores. Based on the viscous zone model, Song et al. (2021) simulated the coupling mechanism of stress and seepage during SC-CO_2 and hydraulic fracturing. The viscosity of CO_2 is low, which is easy to compensate for the pressure loss caused by filtration. It avoids the sensitive behavior of pore pressure and effective stress to filtration, and promotes the expansion of fracture width. Zhou and Burbey (2013) studied the influence of fluid properties on fracture propagation behavior by using cohesive zone model and pore elastic model. It was found that fluid viscosity was a very important characteristic, which greatly affected the penetration rate and permeability coefficient of fracturing fluid. The influence of viscosity can even dominate and exceed the influence of compressibility. Table 1 is the effect of SC-CO_2 low viscosity characteristics on the initiation and propagation of rock fractures. Besides, the low viscosity of SC-CO_2 can also effectively solve the problem of blocking flow and desorption (Clarkson and Bustin, 2000), which is conducive to improving oil recovery.

In Table 1, SC-CO_2 is compared with traditional liquids (such as water and oil) for fracturing. The results showed that SC-CO_2 can reduce the fracture pressure of rock due to its low viscosity. It is found that the use of SC-CO_2 as a fracturing fluid can form a more complex and extensive fracture network through AE monitoring, fracture CT scanning, microscopic inference and other techniques. It can be better connected with natural fractures and rock bedding, thereby improving the fracturing efficiency.

2.1.2. Surface tension effect of supercritical CO_2

SC-CO_2 has an extremely low surface tension, so it is easy to flow in the pores. It can enter any space larger than CO_2 molecules, thereby increasing its stress intensity factor (D.W. Zhou et al., 2019). In the process of fracture initiation, the surface tension of fracturing fluid controls the fluid to enter the pore space or micro-fracture, which reduces the effective stress around the bottom hole (Meng et al., 2019). For a specific pore structure, the breakthrough pressure is determined by the interfacial tension (σ) and the contact angle (θ):

$$P_c = \frac{4\sigma \cos\theta}{d} \tag{1}$$

where P_c represents the breakthrough pressure (MPa), σ is the interfacial tension (mN/m), θ is the contact angle (°); d is the critical pore size (m) that the fluid can enter (Espinoza and Santamarina, 2010).

Espinoza et al. found that the contact angle of SC-CO_2 in shale is close to 0°, while the contact angle of water was 15°. When the pressure was greater than 10 MPa, the interfacial tension of SC-CO_2 was about 20–30 mN/m, and the interfacial tension of water was 50–70 mN/m (Espinoza and Santamarina, 2010; S. Wang et al., 2016). In Eq. (1), when SC-CO_2 and water are in relatively homogeneous shale, the initiation pressure required for SC-CO_2 fracturing is less than that for water-based fracturing. In order to test the dependence of the fracture pressure on the fluid interfacial tension, J.H. Wang et al. (2017) used the invasion pressure to describe the response of the borehole wall to the injected fluid. The invasion pressure is defined as the minimum pressure required to overcome the capillary force, and force the fluid to enter the pore space through the maximum available pore throat. The relationship between invasion pressure and interfacial tension can be expressed by Leverett *J*-function, which is defined as:

$$J = \frac{P_c}{\sigma}\sqrt{\frac{k}{\Phi}} \tag{2}$$

In the formula, J is a function; P_c is the invasion pressure (MPa); σ is the interfacial tension (mN/m); k is permeability (mD); Φ is porosity (Gan et al., 2015).

As shown in Eq. (2), the invasion pressure is only controlled by interfacial tension, and has nothing to do with fluid compressibility. Moreover, as the temperature increases, the surface tension gradually decreases. When the temperature is close to the critical temperature of CO_2, the surface tension drops to zero (Zhuang et al., 2023). This makes it easy for SC-CO_2 to penetrate and diffuse into the solute micropores, which is conductive to the improvement of mass transfer rate.

The physical properties of SC-CO_2 are one of the most critical reasons for the reduction of fracture initiation pressure and the generation of micro-cracks in shale samples (Chen et al., 2019), which have an important influence on fracture initiation and propagation. These characteristics influence each other, which determines the role of SC-CO_2 in shale, and then affects the effect of fracture initiation and propagation.

2.1.3. Penetration and diffusion effect of supercritical CO_2

When SC-CO_2 is injected into the shale formation, it can quickly fill the pore space due to its high penetration capacity. The increase of the number of molecules in the pores of the rock causes high pressure, which promotes the stress failure of the rock. This penetration capacity and diffusion ability enables SC-CO_2 to effectively reduce the initiation pressure of shale, which will fill and expand fractures. During multi-layer fracturing, with the increase of the ratio of horizontal permeability to vertical permeability, the productivity also gradually increases (H.L. Liu et al., 2018). At high temperature, the mobility of SC-CO_2 molecules is enhanced, then diffusing into rock fractures. The induced fractures will continue to break and expand to the rock boundary when the temperature decreases. With the fracture size increases, the required expansion pressure decreases. The expansion of CO_2 helps to alleviate the fluid pressure decrease and further promote fracture propagation (L. Wang et al., 2017). Choi et al. conducted non-Darcy flow tests, and considered the inertial effect to detect the penetration capacity of SC-CO_2 using the Forchheimer formula (Choi et al., 2017). It was found that the change of permeability was affected by pore pressure. Ito (2008) proposed an initiation criterion considering the effect of fracturing fluid infiltration on pore pressure when calculating the initiation pressure:

$$\sigma\theta|r = R + d = \sigma \mathrm{t} \tag{3}$$

where σ_θ is the effective circumferential stress (MPa), R is the borehole radius (m), d is the characteristic length of rock tensile failure (m), and σ_t is the tensile strength of rock (MPa) (L.Q. Chen et al., 2015).

They believed that this criterion is a general formula of fracture initiation criterion considering pore pressure. SC-CO_2 penetration not only changes the pore pressure field, but also causes mechanical rock damage due to its adsorption, resulting in lower breakdown pressure (L.Y. Liu et al., 2018). Moreover, X.X. Zhang et al. (2017) used numerical simulation to propose a complex parameter to represent the comprehensive effect of shale permeability, fluid viscosity and pressurization rate. It was found that with the increase of complex parameters, the initial pressure of fracturing decreased and the seepage area increased. In shale fracturing experiments, Jia et al. (2018) found that the fracturing fluid with lower viscosity will lead to a greater diffusion depth around the injection wellbore and natural microcracks, as shown in Fig. 1. The penetration capacity and diffusion of SC-CO_2 can also change the viscosity and surface tension of pore fluid, which further affects the fluidity of oil and gas in shale.

2.1.4. Dissolution effect of supercritical CO_2

When SC-CO_2 penetrates into the reservoir, CO_2 will dissolve into shale pore water to form carbonic acid (H_2CO_3). In the absence of buffer substances in the solution, it will lead to a significant decrease in pH value (Alemu et al., 2011; Rempel et al., 2011; K.R. Wang et al., 2016). The diffusion of carbonic acid into carbonate minerals will trigger a series of chemical reactions, which will lead to the dissolution of minerals and cause a large number of etching

Table 1
Effect of viscosity of $SC-CO_2$ fracturing fluid on rock.

Sample type	Fracturing fluid type	Experimental method	Research results	References
Granite	$SC-CO_2/L-CO_2$	AE monitoring	The viscosity of $SC-CO_2$ is lower than that of $L-CO_2$, which will produce three-dimensional extended fractures, while $L-CO_2$ extends along the plane.	Ishida et al. (2012)
Granite and tuff	$SC-CO_2$/Water	3D fracture geometry	The propagation of fractures is significantly affected by the viscosity of fracturing fluid, the viscosity of water is 25 times that of $SC-CO_2$. The fractures formed by $SC-CO_2$ are more complex than those formed by water.	Kizaki et al. (2013)
Granite	$SC-CO_2$/Water/ Viscous oil	AE monitoring	Fracturing mode is affected by the viscosity of fracturing fluid. $SC-CO_2$ low-viscosity fluid can cause shear-dominated fracture, which can produce multiple branches of extensive and complex fractures.	Inui et al. (2014)
Granite	$SC-CO_2$/Water/Oil	AE monitoring; Fluorescence observation method; Image analysis	The curvature is defined as the total fracture length along a path divided by the direct length at both ends of the fracture. When a low-viscosity fluid ($SC-CO_2$) is injected, the curvature is 1.13. When a high-viscosity fluid (oil) is injected, the curvature is 1.05, indicating that the viscosity of the fracturing fluid affects the fracture propagation mode.	Y.Q. Chen et al. (2015)
Granite	$SC-CO_2/L-CO_2$/ Water/Viscous oil	AE monitoring; Microscopic inference	The initiation pressure of $SC-CO_2$ is lower than that of $L-CO_2$, water and viscous oil. The distribution of AE sources indicates that the use of low-viscosity fluid fracturing caused three-dimensional bending fractures with many secondary branches.	Ishida et al. (2016)
shale and sandstone	$SC-CO_2/L-CO_2$/ Water	AE monitoring; CT scan of fracture; DR scan	The initial fracturing pressure of $SC-CO_2$ is about 15% lower than that of $L-CO_2$ and about 50% lower than the pressure required for hydraulic fracturing. This is due to the low viscosity characteristics of $SC-CO_2$. The fracture width induced by $SC-CO_2$ is larger than that induced by hydraulic fracturing, which is more likely to be connected with natural fractures and bedding.	X.W. Zhang et al. (2017)
Tight sandstone	$SC-CO_2/L-CO_2$/ Water	Fracture analysis	$SC-CO_2$ has low viscosity characteristics, resulting in a 28.2% reduction in fracture initiation pressure compared with slick water, and $L-CO_2$ fracture initiation pressure is 22.1% lower than that of slick water.	Ye et al. (2018)
Tight sandstone	$SC-CO_2$/Slick water/ Guar gum	Fracture CT scan	In the process of fracturing, with the decrease of fluid viscosity, the initiation pressure also decreases. it is confirmed that the low viscosity fluid produces more branch fractures.	Zou et al. (2018a)
Shale	$SC-CO_2$/Water	Penetration testing; Profilometer scanning	Compared with water, the viscosity of $SC-CO_2$ is lower, and it is easier to reach the fracture tip and penetrate into the shale matrix, resulting in more complex stress field at the fracture tip.	Jia et al. (2018)
Shale	$SC-CO_2$/Water	SEM scanning; Stereoscopic microscope monitoring	Because the viscosity of $SC-CO_2$ fracturing fluid is lower than that of fresh hydraulic fracturing fluid, the initiation pressure of $SC-CO_2$ is smaller. $SC-CO_2$ has a greater ability to enter micropores or microcracks, which can produce more complex fractures.	He et al. (2019)
Shale	$SC-CO_2/CO_2$ foam/ $L-CO_2$/Slick water	–	The viscosity of $SC-CO_2$ fluid is low and the diffusion coefficient is large, which will significantly reduce the initiation pressure. The initiation pressure is from small to large: $SC-CO_2 < L-CO_2 < CO_2$ foam < slick water.	Zuo et al. (2021)
Shale	$SC-CO_2$/Water	–	The $SC-CO_2$ fluid has a lower viscosity than water, resulting in a $SC-CO_2$ fracture pressure of 12.3 MPa and a hydraulic fracture pressure of 23.8 MPa. The $SC-CO_2$ fracturing fluid can penetrate into the unit near the main fracture to activate more natural fracture.	Yin et al. (2024)

holes. This changes the mechanical properties of rock, making shale more fragile (Memon et al., 2024; Zou et al., 2018b). Tao et al. (2024) used Berkovich indenter to analyze the micromechanics of shale, the indentation position and corresponding micromorphology were studied by scanning electron microscope (SEM). The results showed that after CO_2 treatment, a large number of dissolved pores were generated in the shale matrix. The weak surface of the structure was opened, resulting in the formation of new fractures. At the same time, the micro-elastic modulus and hardness of shale decreased by 51.3% and 63.3% respectively. Based on scanning electron microscope imaging and energy spectrum, Tian et al. (2020) treated Longmaxi shale with carbonic acid for 48 h. It was found that the dissolution of calcite and dolomite by carbonic acid led to the existence of dissolution pits, and the elastic modulus and hardness were reduced by 17.3% and 34.8%, respectively. On the basis the research of Tian et al. (2020), Cheng et al. (2022) further analyzed the load-displacement curves of individual minerals treating Longmaxi shale samples in $SC-CO_2$-water environment for 3 months. It was observed that quartz was the least affected mineral, and carbonate and clay minerals were the most affected by the treatment. The elastic modulus of clay decreased by 38.2%, followed by the elastic modulus of dolomite decreased by 24.45%. The elastic modulus of calcite decreased by 5.18%. In a similar study, Shi et al. (2020) found that the overall mechanical strength of shale samples decreased after exposure to $SC-CO_2$-water. The hardness, elastic modulus and fracture toughness decreased by 29.5%, 11% and 11.3%, respectively. Compared with quartz-rich areas, the mechanical effects of clay-rich areas are significantly weakened. On the other hand, mineral dissolution can expand pores and increase permeability. Jia et al. (2018) compared hydraulic with $SC-CO_2$ fracturing. The results showed that $SC-CO_2$ fracturing can strip mineral particles from the fracture surface. Under the same stress conditions, $SC-CO_2$ fracturing increases shale permeability by 5 orders of magnitude, which is about 3 orders of magnitude higher than hydraulic fracturing. Hashemi and Zoback (2021) measured the fracture permeability of samples with high carbonate content. It was observed that after 3.5 days of interaction between the sample and $SC-CO_2$, due to the dissolution of carbonates, shale permeability and fracture surface degradation increased. Pan et al. focused on the pore structure, using a variety of methods such as high-pressure mercury intrusion porosity test (Pan et al., 2018b). It was observed that after the continental shale was exposed to $SC-CO_2$ for two weeks, the number of micropores and mesopores increased with the increase of macropores, resulting in an increase in porosity and permeability. Yasuhara et al. applied normal effective stress to fractures in another experiment (Yasuhara et al., 2011). It was pointed out that the change of pore size may be caused by the combined action of mechanical crushing and chemical dissolution of contact particles. As the saturation time becoming longer and longer, CO_2 causes more pores to form in the interior. These additional pores will form a secondary pore system, thereby weakening the strength of the natural pore structure, so the strength of the rock after saturation treatment will decrease (Marbler et al., 2012; Rathnaweera et al., 2015).

In addition, carbonic acid can also react with silicate minerals in shale to precipitate into solids, making the permanent storage of CO_2. Gunter et al. conducted geochemical experiments involving CO_2 and rock under conditions of 105 °C and 9 MPa for 30 days. It

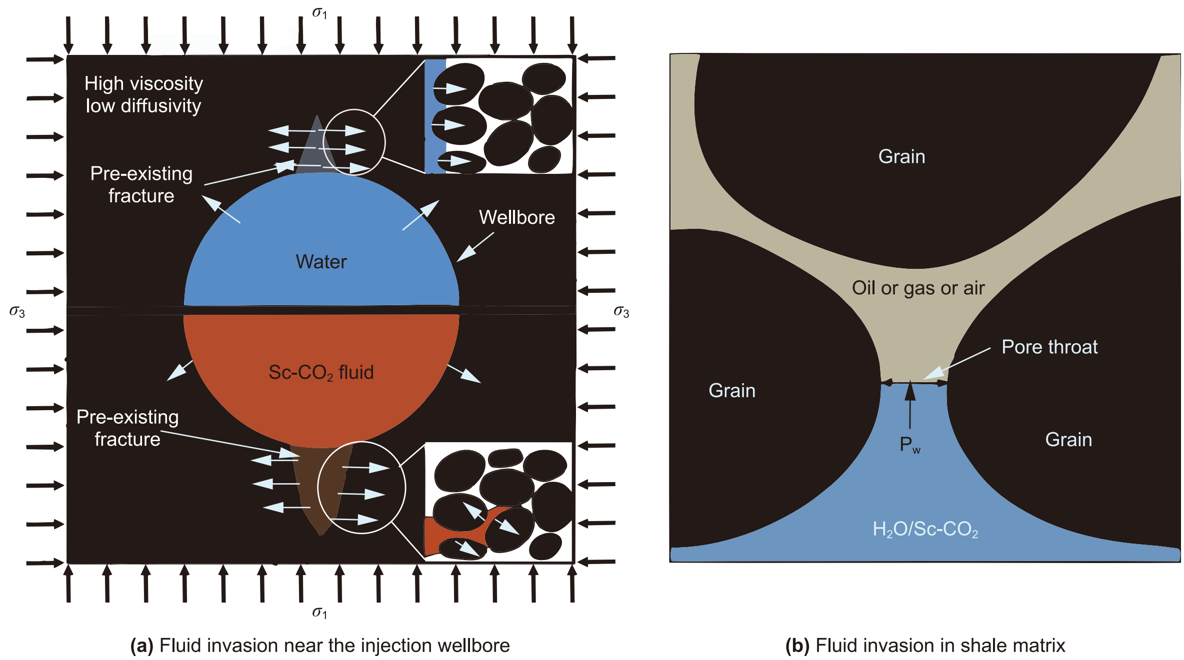

Fig. 1. **(a)** Fluid intrusion near the injection wellbore. **(b)** In the region far from the injection wellbore (Jia et al., 2018).

was found that as time extended, the decomposition of illite and chlorite on the rock surface or pores became more pronounced. The precipitation of dolomite, calcite, magnesite, and siderite was also more readily observed (Gunter et al., 1997). J. Lu et al. (2016) found that after shale was exposed to SC-CO_2-salt water, the most significant change was the dissolution of carbonate minerals. Especially calcite, a small amount of calcite precipitates on the reaction surface and pores, followed by dolomite. Wang et al. found that in the CO_2-water-shale interaction, mineral dissolution and new mineral precipitation were closely related to the formation of carbonic acid and electric dissociation. The dissolution of feldspar, silica and clay minerals increased with increasing temperature. It was found that the generated gibbsite supported the feasibility of China's first CCS project to storage CO_2 through mineralized geology (Wang et al., 2013). Although the chemical reaction of CO_2 with water and rocks makes mineral components precipitate and realize mineral storage. However, the precipitation of new minerals will lead to the decrease of rock permeability. Yu et al. (2012) found that minerals such as potassium feldspar, albite, calcite and ankerite were dissolved to different degrees after SC-CO_2 experiments through core scanning electron microscopy and XRD analysis. After dissolution, these minerals lead to the precipitation of new minerals and the release of clay particles formed by acid-salt cements. These particles are transported and accumulated in the pore throat during fluid flow, resulting in a significant decrease in core permeability. Therefore, it is necessary to comprehensively consider the influence of the interaction among CO_2, water and rock on the initiation and propagation of fractures in shale reservoirs.

2.1.5. Adsorption effect of supercritical CO_2

The dissolution of CO_2 in shale reservoirs is accompanied by the adsorption of CO_2 on the surface of shale, which may cause volumetric strain and reduce rock strength. This may have a positive impact on hydrocarbon development (Ao et al., 2017, 2020; Lyu et al., 2015; S. Wang et al., 2019). According to previous studies, there are two ways that gas adsorption affects shale. First, the adsorption of CO_2 increases the expansion strain on the shale surface (Sun et al., 2024b). The swelling caused by adsorption will narrow the pores, thus transforming the macropores into mesopores, which cause the expansion of the rock matrix to generate fracture closure or permeability reduction (Bhuiyan et al., 2020; Cheng et al., 2020; Hui et al., 2019; Pan et al., 2018a). Memon et al. (2022) performed 3D fracture segmentation and aperture measurement on X-ray CT scans of natural fractures before and after fracturing. Fig. 2(a, b) shows the average decrease in fracture width before and after SC-CO_2 fracturing. In order to verify the visual observation results, the number of voxels contained in the two segmented fractures was calculated using the material statistics option. It was found that before and after CO_2 fracturing, the number of voxels of the two fractures generally decreased by 19%–35%, as shown in Fig. 2(c and d), indicating that there will be fracture closure or shrinkage after SC-CO_2 fracturing. Combined with the expansion of natural fractures observed after SC-CO_2 treatment test, it is confirmed that the expansion of shale matrix reduces the conductivity of the channel between fractures. Wu et al. (2017) evaluated the effect of CO_2 exposure on the permeability of Utica shale samples through pressure pulse attenuation experiments. It was found that the pore wall expansion caused by CO_2 adsorption reduced the flow path of the fluid, resulting in a decrease in the porosity and permeability of different shale samples. Busch et al. (2016) also drew the same conclusion by exploring the interaction between clay minerals and CO_2. Montmorillonite can adsorb a large amount of CO_2, which may lead to volume expansion. Subsequently, expansion pressure was generated, resulting in fracture closure or fracture porosity reduction. Furthermore, the adsorption of CO_2 and the chemical reaction between shale and fluid decrease the brittleness of shale and increase its plasticity, which increases the initiation pressure of shale (Lyu et al., 2016). Through the above research, it can be seen that the expansion strain caused by shale adsorption has a certain negative effect on the fracture initiation and propagation. However, gas adsorption also changes the mechanical properties of shale, reducing the strength and elastic modulus of shale. According to Gibbs theory (Gibbs, 1967), the pure adsorption of CO_2 will reduce the surface potential energy of shale and promote the expansion of shale matrix. The theory of surface physical chemistry shows that the decrease of solid surface energy will reduce its strength. The formula of surface energy is shown as follows:

$$d\gamma = RT\Gamma d(\ln p) \tag{4}$$

In the formula, $d\gamma$ is the surface energy increment (J/m^2); R is a general gas constant; T is the temperature (°C); Γ is a constant of the irreversible reaction process; p is the actual gas pressure (Pa). The solid surface energy can be written as:

$$\Delta\gamma = \frac{RT}{V_M S}\int_0^P \frac{V}{P}dp \tag{5}$$

Among them $\Delta\gamma$ is the change of surface energy; V_M is the molar volume (L/mol) of gas; S is the surface area (cm^2), V is the adsorption volume (cm^3).

This adsorption causes the change of surface potential energy of shale, which is equivalent to the change of elastic energy of shale. This will lead to the decrease of mechanical strength of shale (Cao et al., 2013). Y.Y. Lu et al. (2016) measured the CO_2 adsorption-induced expansion in shale in the temperature range of 308–348 K. In the transient compression process, the CO_2 adsorbed by shale will cause variation of stresses. During the slow expansion process, CO_2 is slowly adsorbed by the sample, which reduces the potential energy of the shale surface. Lyu et al. used 3D technology, SEM test and EDS analysis on low clay shale samples, and found that the adsorption of CO_2 led to the decrease of uniaxial compressive strength (UCS) and elastic modulus (Lyu et al., 2018). With the change of time, the UCS and elastic modulus of shale samples decreased by 2.96% and 20.23% respectively on the 10th day. After one month, the UCS and elastic modulus of shale samples decreased by 29.95% and 37.79% respectively. Yin et al. (2017) also carried out similar adsorption experiments to test the mechanical properties of shale after 10 days of adsorption. Secondary fractures were generated due to the uneven expansion caused by CO_2 adsorption. Subcritical CO_2 saturation reduced the UCS and elastic modulus of shale by 22.86% and 23.10%, respectively. SC-CO_2 saturation led to the decrease of UCS and elastic modulus of shale by 33.89% and 33.97%. In addition, in the process of fracture initiation, the huge thermal stress generated by CO_2 adiabatic expansion and phase change can significantly increase the damage and failure of rock, which is conducive to the initiation of micro-fractures on the surface of main fractures and further improves the complexity of fracture network (Guo et al., 2022; X.J. Li et al., 2018). The fracture change and rock strength reduction caused by shale expansion strain are interdependent, and this process involves the complex interaction of material mechanics and chemical properties. Therefore, one of the key studies in the future is to optimize the properties of the adsorption medium and its interaction with environmental conditions to be more effectively applied to oil and gas development and reservoir reconstruction.

When CO_2 reacts with minerals in shale, SC-CO_2 will change the porosity, permeability and rock mechanical properties of shale through dissolution and gas adsorption. In dissolution effect, the negative separation pressure and the positive separation pressure represent the adhesion force and repulsive force between the adjacent mineral surfaces, respectively. It can lead to the weakening of the rock by changing the separation pressure from strong negative to weak negative or even positive (Zeng et al., 2020). The expansion caused by adsorption can lead to the further closure of existing fractures. At the same time, it also lead to the redistribution of stress field, thus reducing the strength of rock. Especially after multiple adsorption-desorption cycles, the reduction in strength will make the rock more prone to fracture during fracturing. According to most experimental studies, it is found that the effect of dissolution on shale weakening was more significant than that of CO_2 adsorption. These two mechanisms explain the loss of mineral observed, the increase of pore percentage, the decrease of initiation pressure, and fracture propagation in all treated shale samples (Jiang et al., 2016; C. Qin et al., 2017). It is worth noting that due to the heterogeneity of different shales, the degree of influence of these two mechanisms will be different.

2.2. Influencing factors of fracture initiation and propagation in shale

The initiation and propagation of SC-CO_2 in shale are affected by many factors, including natural factors, such as shale characteristics, bedding planes, natural fractures, and controllable factors, temperature, pressure, CO_2 concentration, and fracturing fluid injection rate and so on. Through detailed analysis of natural factors and reasonable regulation of controllable factors, the effect of initiation and fracture propagation can be optimized, and the utilization efficiency of SC-CO_2 in shale can be maximized.

2.2.1. Shale properties

Shale contains a variety of complex mineral components, such as carbonate, clay (illite, montmorillonite, chlorite), quartz and pyrite (Z.K. Hou et al., 2024). From the perspective of mineral composition of shale, on the one hand, mineral composition can affect the friction characteristics of shale reservoir. Kohli and Zoback (2013) conducted laboratory experiments on natural shale samples from three oil and gas reservoirs, and applied the particle accumulation framework model to explain the control of composition on friction characteristics. It was observed that the friction strength decreased with the increase of clay and organic content, and the debris contact was gradually replaced by clay aggregate contact. The evolution of shale particle stacking framework leads to similar changes in the particle size of bearing components. Therefore, in the process of SC-CO_2 fracturing, different contents of clay and organic matter have different effects on the friction of shale reservoirs. It is necessary to consider that shale friction may cause negative effects during fracture propagation, especially in the case of low content. On the other hand, using mineral components to calculate brittleness is one of the main methods to evaluate shale brittleness. Usually, the combination of elastic modulus and Poisson's ratio is used to characterize the brittleness of shale. The greater the elastic modulus, the lower the Poisson's ratio, and the more obvious the brittle characteristics of the rock is (Qin et al., 2016). In order to improve the accuracy of rock brittleness, Luo et al. proposed a new method for calculating brittleness BIEMS (brittleness index is composed of elastic parameters, mineral content and in-situ stress conditions) (Luo et al., 2024):

$$\mathrm{BIEMS} = \frac{V_{QA}\times B_{QA} + V_{DO}\times B_{DO} + V_{PY}\times B_{PY} + V_{FD}\times B_{FD} + V_{CA}\times B_{CA}}{\alpha_p} \tag{6}$$

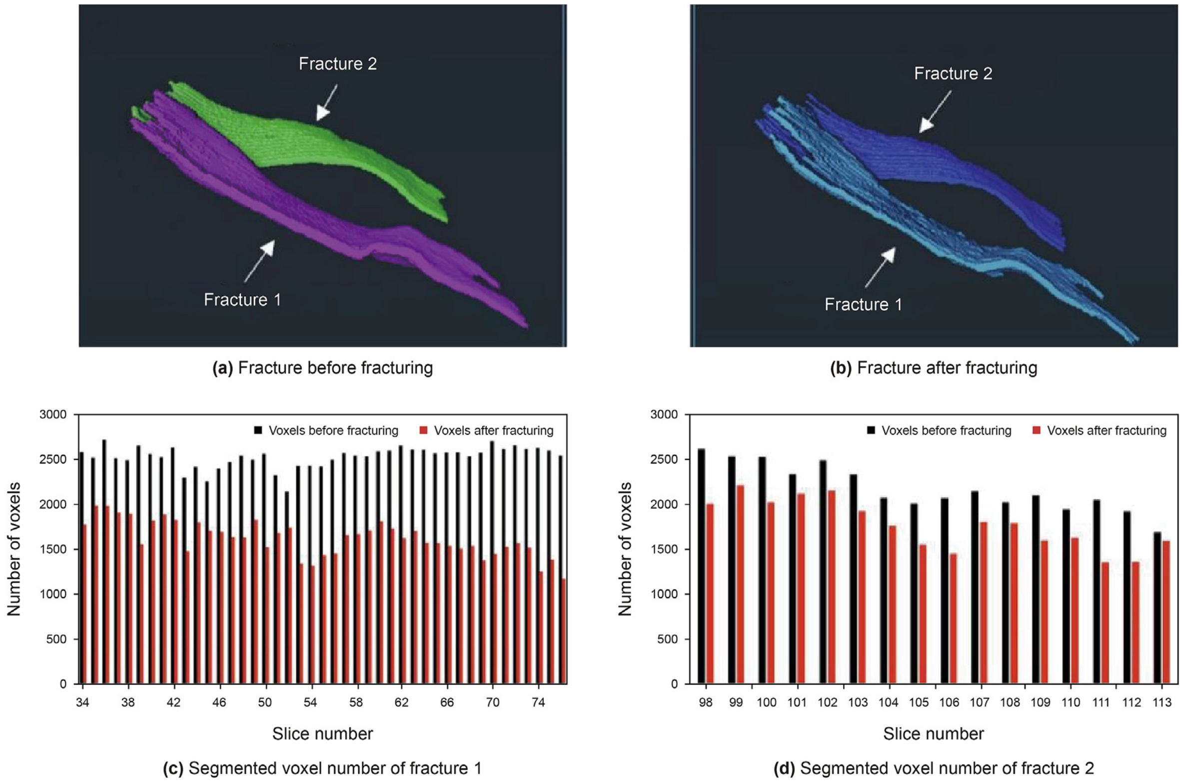

Fig. 2. Fracture comparison before and after fracturing (Memon et al., 2022).

$$\alpha_p = \frac{P_0 - P_f}{P} \tag{7}$$

In Eq. (6), V_{QA}, V_{DO}, V_{PY}, V_{FD} and V_{CA} are the relative percentage content of quartz, dolomite, pyrite, feldspar and calcite, respectively. B_{QA}, B_{DO}, B_{PY}, B_{FD} and B_{CA} are the inherent brittleness values of quartz, dolomite, pyrite, feldspar and calcite. In Eq. (7), α_p is the condition coefficient of ground stress; P_0, P_f and P are overburden pressure, pore pressure and confining pressure (MPa), respectively.

By combining the optimized logging interpretation results with the field measured data such as relative mineral content, overburden pressure, pore pressure and confining pressure, the dynamic brittleness index is calculated by Eqs. (6) and (7). The obtained brittleness index can be used to establish the continuous brittleness profile of the reservoir. In the process of fracturing, the mineral composition is reduced through the chemical reaction of CO_2 and shale. The brittleness of rock is also increased, so as to achieve the purpose of reducing the fracture pressure of shale. Wang et al. (2021) studied the influence of shale microstructure and mechanical parameters through the indoor rock-fracturing fluid immersion test system. The results showed that the brittleness of shale after SC-CO_2 immersion was increased by 40%–50% compared with that after slick water immersion, which was beneficial to improve pore penetration and reduce fracture pressure.

In addition to the mineral composition, the confining pressure, pore size and distribution inside the shale play an important role in the SC-CO_2 fracturing process. Wang et al. used different triaxial stresses to study the induced fracturing of fracture shale injected with SC-CO_2 (L. Wang et al., 2017). Through X:Y:Z = 1600:2100:2600, X:Y:Z = 1100:1600:2100 and X:Y:Z = 1200:2100:3000 three different confining pressures on shale fracturing, it was found that reducing the triaxial stress level and increasing the stress difference will reduce the shale fracture pressure. When the minimum horizontal stress is not perpendicular to the pre-existing fractures, the triaxial stress may become the dominant position in the fracturing process. Zhao et al. observed the sample image through emission scanning electron microscope (Zhao and Yu, 2017). Some pore sizes were marked, and the average pore radius and the most probable pore radius (maximum probability pore radius) of core samples were obtained. It was found that the breakthrough pressure during SC-CO_2 fracturing decreased in a power function with the increase of the average pore radius or the most likely pore radius. Yin et al. (2016) used XRD, N_2GA and fractal theory to study the microstructure characteristics of shale before and after SC-CO_2 treatment. It was found that the specific surface area of shale decreased, the number of micropores decreased significantly and the average pore diameter increased after the action of SC-CO_2. The pore structure of shale changed from complex to smooth. The reason of pore change was explained by the dissolution and adsorption expansion mechanism of SC-CO_2. Zhou et al. (2020) analyzed the shale samples before and after pure water and CO_2-water by XRD, NMR and fractal analysis. After CO_2 came into contact with water, with the increase of CO_2 pressure, the content of quartz in shale increased, while the content of carbonate and clay minerals decreased. Meanwhile, the porosity increased from 2.88% to about 3.16%, the connectivity of pores was improved, micropores and mesopores were gradually transformed into macropores. Lu et al. (2019) conducted nuclear magnetic resonance, uniaxial compressive strength and acoustic emission tests on shale samples from the Sichuan Basin before and after CO_2 saturation. It was found that the change in the volume ratio of mesopores of 10–50 nm was positively correlated with mechanical properties, while the change in the volume ratio of macropores greater than 250 nm was negatively correlated with mechanical properties. The change of pore size distribution is considered to be one of the main reasons for the deterioration of mechanical properties of shale after CO_2 saturation. Under the action of load, the stress concentration is easy to occur at the edge of the large hole, resulting in fracture initiation. Under continuous loading, the fracture propagation eventually leads to the failure of the specimen.

The mineral composition of shale, such as clay and organic matter, affects its friction characteristics, resulting in the decrease of friction strength with the increase of content. The brittleness index calculated by mineral composition and in-situ stress conditions can be used to evaluate the brittleness of rocks, thus predicting the fracturing effect. Moreover, confining pressure, pore size and distribution also have significant effects on SC-CO_2 fracturing.

2.2.2. Beddings and natural fractures

Researchers' study on the mechanical properties of shale shows that the compressive strength of anisotropic shale varies with the change of bedding direction (Hou et al., 2015; Yan et al., 2014). The fracture initiation pressure and fracture propagation of shale will vary greatly with the change of bedding orientation. Table 2 summarizes the fracture initiation pressure and fracture morphology of shale under different bedding angles (Zhang et al., 2019). In general, the initiation pressure decreases with the increase of the bedding angle, and the fracture morphology changes with the bedding angle. Chen et al. (2024) also conducted a similar experiment, by comparing the fracture initiation pressure and fracture pressure of SC-CO_2 fracturing at different bedding angles. It can be seen that the average fracture initiation pressure and fracture pressure of layered shale were reduced by 6.15 and 8.97 MPa respectively. J.M. He et al. (2020) used water and SC-CO_2 to study the mechanical response and fracture propagation of shale fractures. It was observed that the fracture width (including maximum width and opening width) of SC-CO_2 fracturing was larger than that of hydraulic fracturing with bedding angles of 0 and 90. Because after the fracture initiation, the volume expansion of SC-CO_2 is more significant, which leads to the increase of fracture width. Fracture propagation is not only affected by the bedding angle, but also controlled by the microscopic mechanical properties of the bedding plane. The bedding plane can lead to fractures or weak cementation surfaces in the rock layer, which affect the formation of fracturing fractures (Li et al., 2015; Zhang et al., 2020; J. Zhang et al., 2021). Jiang et al. (2018) used different triaxial stresses to combine acoustic emission monitoring and CT scanning during SC-CO_2 fracturing. The initial position, propagation direction and number of fractures were analyzed. It was observed that the fracture distribution was usually random and spread along the weak structural plane of shale or the existing fracture direction, as shown in Fig. 3. The elastic modulus between single layers is within the critical value, and fractures will extend along the layers. This critical value can control the fracture propagation behavior of layered strata (W. Zhou et al., 2022). Based on XRD and SEM experiments, Li et al. (2022) studied the dissolution of minerals and the changes of pore structure before and after CO_2 injection. Experimental results showed that the viscosity of CO_2 was low, and the bedding plane was easy to open. The longitudinal fractures intersected with the bedding plane, forming a complex fracture network. In the process of CO_2 fracturing of thin interbedded shale, the horizontal principal stress difference is no longer the key factor to form a complex fracture network, while the vertical stress and natural fractures play an important role.

There are natural fractures in the shale, which are the existing fractures in the rock. When SC-CO_2 enters the shale, it will preferentially enter and expand along the path of natural fractures. SC-CO_2 can better penetrate narrow pores and tiny natural fractures, and form a complex cross network with natural fractures (X.J. Li et al., 2018). The application of fracturing technology to activate natural fractures is considered to be the key to the formation of complex fracture networks in unconventional tight reservoirs (Cong et al., 2022; Zhang et al., 2021; Zhang and Li, 2016). Guo et al. (2022) compared three kinds of natural fractures with different densities in the numerical simulation study of fracture initiation and propagation. It was observed that SC-CO_2 can easily penetrate into natural fractures and further cause fractures. As shown in Fig. 4, the better the development of natural fractures, the higher the complexity of fractures are, while the low-density natural fractures hinder the further communication between SC-CO_2 and natural fractures. Suo et al. (2024) used prefabricated natural fractures and studied the relationship between SC-CO_2 and natural fractures through single factor variable control experiments. When the angle between natural fracture and SC-CO_2 fracturing fracture was 30°, many cross fractures were formed. When the intersection angle was 45°, shear fractures and through fractures were formed. When the intersection angle was 60°, there were more shear fractures in the development process. Based on the simplified three-dimensional displacement-discontinuity method, Zhao et al. (2021) carried out a series of fracturing experiments of single and multiple fractures. Figs. 5 and 6 show that in natural fractured reservoirs, and SC-CO_2 fracturing can activate more natural fractures to connect with each other and produce larger stimulated reservoir volume compared with slick water and gel-induced fractures. Whether single fracturing or multiple fracturing, the natural fracture volume of SC-CO_2 fracturing is always several times that of slick water fracturing and gel fracturing.

In practice, the pre-existing faults, fractures and weak layer interfaces have a great influence on the propagation of fractures. According to the bonding strength and direction of fractures or interfaces, the propagation of fractures may be inhibited, promoted, prevented or reoriented. Therefore, in view of the current development difficulties of shale reservoirs, combined with the existing understanding of SC-CO_2 fracturing fracture propagation, the research on 3D fracture propagation induced by SC-CO_2 under heterogeneous conditions such as natural fracture, bedding direction, layered reservoir and stress should be strengthened in the future. The fracture characteristics are reconstructed and quantitatively evaluated. Numerical simulation methods such as extended finite element and discrete element are used to quantitatively analyze the influence law of multi-field coupling in order to optimize the fracture propagation effect.

2.2.3. Proppant transport

When high pressure is applied, CO_2 interacts with fluids and minerals in shale, resulting in rock fracture and pore expansion. This expansion can form the main fractures, but also can form many fine branch fractures. The formation of fractures provides sufficient fracture space for proppants, also provides long-term fracture conductivity and efficient artificial channels for oil and gas flow and fluid heat exchange (Cipolla et al., 2008; King, 2010; Liang et al., 2016).

In the process of fracturing fluid injection, SC-CO_2 will drive proppant to move to the fracture, and the distribution of proppant in complex fracture network will have a great impact on fracture propagation (Sun et al., 2024a). Therefore, according to the morphological characteristics of fractures, Zheng et al. (2022c) designed an experimental system to study the transport of proppant in fractures. It was considered that the migration of proppant along the top of sand dune to the depth of fracture was the main mechanism of SC-CO_2 migration in flat fracture. After the proppant was added, and the unsupported fluid was continuously injected. The wave-like moving layer was formed on the surface of the sand dune. The proppants was transported into the deeper fractures, so as to support the existing fractures and generate more staggered

Table 2
Fracture pressure and propagation of shale under different bedding angles.

Fracturing fluid pattern	Stratification angle, °	Deviatoric stress, MPa	Confining pressure, MPa	Injection rate, mL/s	Fracture pressure, MPa	Shale fracture morphology map
SC-1	0°	25	20	0.2	40.51	
SC-2	45°				35.89	
SC-3	60°				32.31	
SC-4	90°				31.09	
SC-5	0°	25	20	0.3	52.15	
SC-6	45°				39.94	
SC-7	60°				44.46	
SC-8	90°				38.04	

and complicated branch fractures. Compared with flat fracture, Zheng et al. (2022a) analyzed the transport and placement characteristics of proppant in curved fracture by using laser morphological scanning technology and computational fluid dynamics (CFD) and the discrete element method (DEM) method. It was observed that the flow path of $SC\text{-}CO_2$ liquid proppant carried in tortuous fractures was tortuous and diversified, and the proppant presented stronger fluctuations and jumps horizontally and vertically during its transportation. Secondly, the position shape of the proppants in the tortuous fractures shows a non-uniform distribution of waves or even aggregation. It shows that $SC\text{-}CO_2$ proppants are more active in the transportation process of tortuous fractures, which makes the fracture network more complicated. H.Z. Wang et al. (2018) used computational fluid dynamics method to simulate the proppant transport of $SC\text{-}CO_2$ in three types of fractures: plane fracture, T-shaped fracture and cross fracture. In the case of plane fracture, with the continuous injection of $SC\text{-}CO_2$ proppant, some sand grains settle at the bottom of the fracture to form sand dunes. Turbulence may be formed at the junction of T-shaped fractures and cross-shaped fractures. The proppants inside the induced fracture in the T-type fracture will further expand to the natural fracture, which will support and expand natural fractures. For cross-shaped fractures, proppants form a small sand dune downstream of induced fractures, which does not promote the possibility of fracture propagation.

Zheng et al. (2024) used computational fluid dynamics combined with discrete element method to study the migration of proppants in rough fracture networks on the surface characteristics

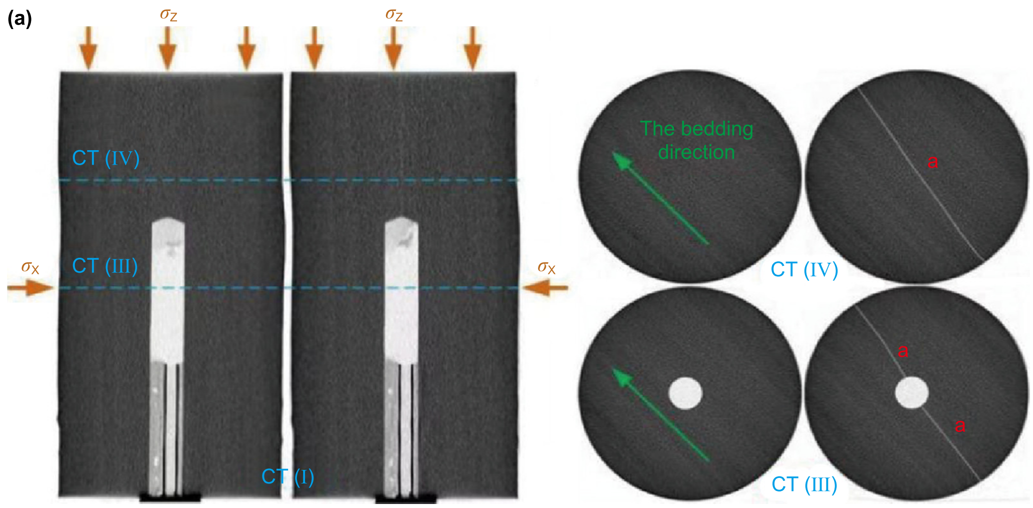

(a) CT (I) is the longitudinal profile image of shale samples. CT (III) and CT (IV) are the transverse profile images of shale samples. a represents parallel bedding fractures.

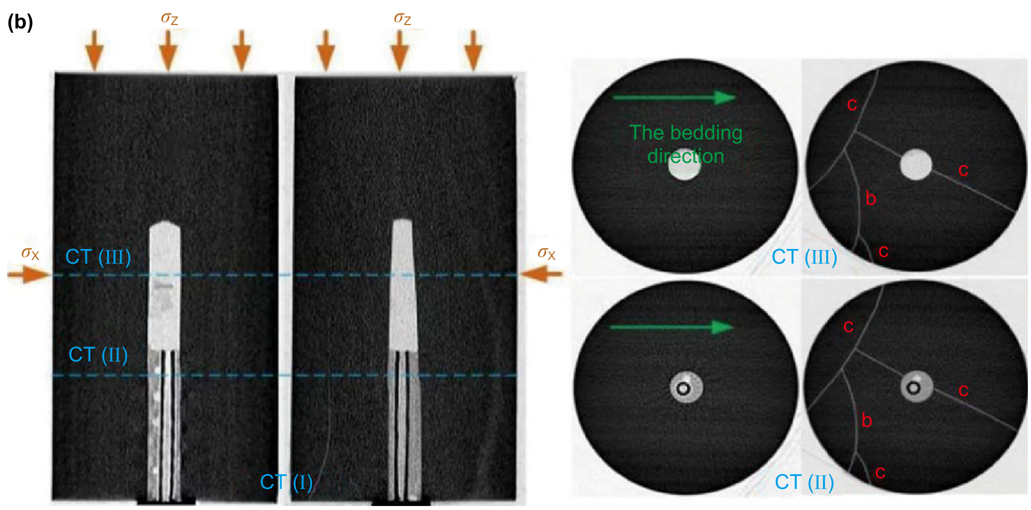

(b) CT (I) is the longitudinal profile image of shale sample. CT (II) and CT (III) are the transverse profile images of shale sample. b indicates that the fracture is perpendicular to the bedding. c represents a certain angle between fracture and bedding.

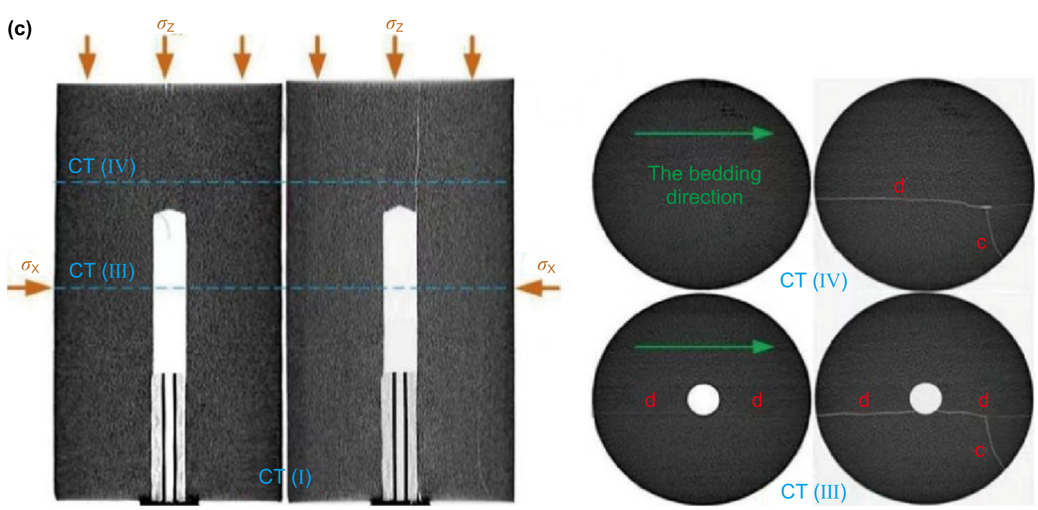

(c) CT (I) is the longitudinal profile image of shale samples. CT (III) and CT (IV) are the transverse profile images of shale samples. d is the natural fracture.

Fig. 3. Relationship between fracture propagation direction and bedding angle (Jiang et al., 2018).

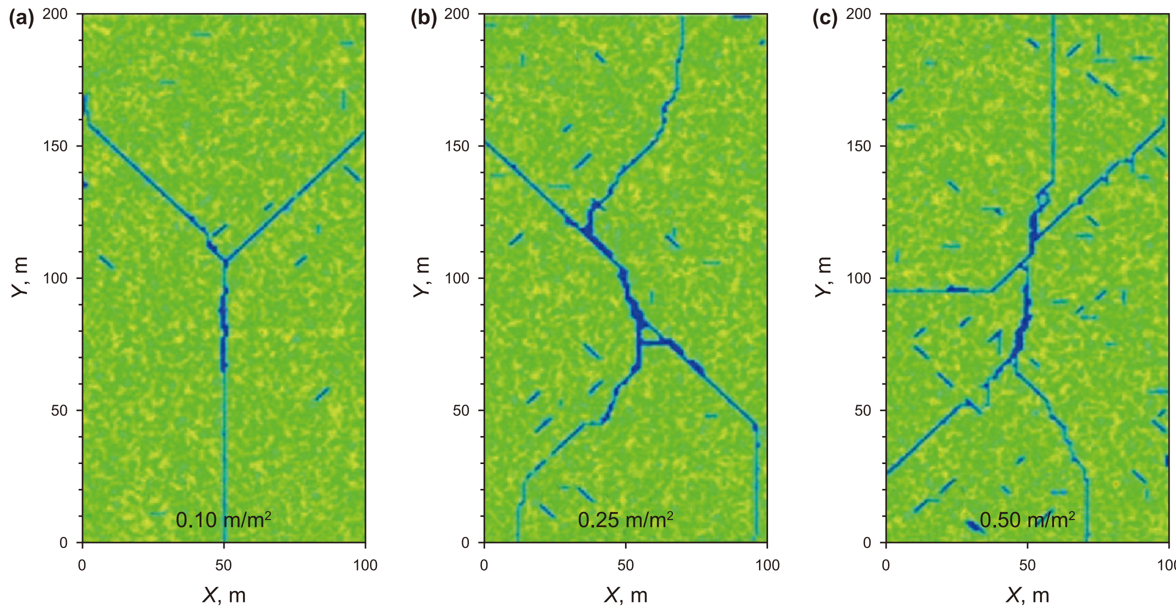

Fig. 4. Influence of natural fracture density on fracture expansion effect (Guo et al., 2022).

of fractures. The transport characteristics of proppant particles in smooth and rough fracture networks were compared and analyzed. It was shown that the irregular shape of the main fracture channel in the rough fracture network enhanced the lateral movement of proppant and improved the possibility of proppant entering the secondary fracture, as shown in Fig. 7. At the same time, the bending of branch fractures, irregular entrance interface and the influence of fracture surface structure in rough fracture network will induce proppant to transfer to branch fractures when flowing at low speed, and then produce more secondary fractures. SC-CO_2 entering shale reservoir can form a complex fracture network. These fractures not only provide space for proppant transportation, but also affect the distribution and transportation path of proppant in the fractures. Especially in curved or irregular fractures, proppant presents stronger fluctuation and uneven distribution, which further increases the complexity and activity of fracture network.

2.2.4. Temperature and pressure conditions

In the process of SC-CO_2 fracturing, temperature and pressure are closely related factors in the process of shale fracturing, which directly affect the fluidity of fracturing fluid, the mechanical properties of rock and the effect of fracture formation and propagation. D.W. Zhou et al. (2019) proposed a fracture mechanics model combined with thermoelastic stress to predict the breakdown pressure. Through the experimental observation of CO_2 between 25 and 100 °C, it was found that the breakdown pressure decreased linearly with the increase of temperature. In order to explore the effect of temperature on SC-CO_2 fracturing, Isaka et al. conducted experiments on hot dry rocks at different temperatures (Isaka et al., 2019). The conclusion showed that the temperature difference between the cold fracturing fluid and the hot rock led to the thermal stress induced by low temperature, which helped to reduce the fracture initiation pressure. The density of induced fractures also decreases. However, as the temperature increases,

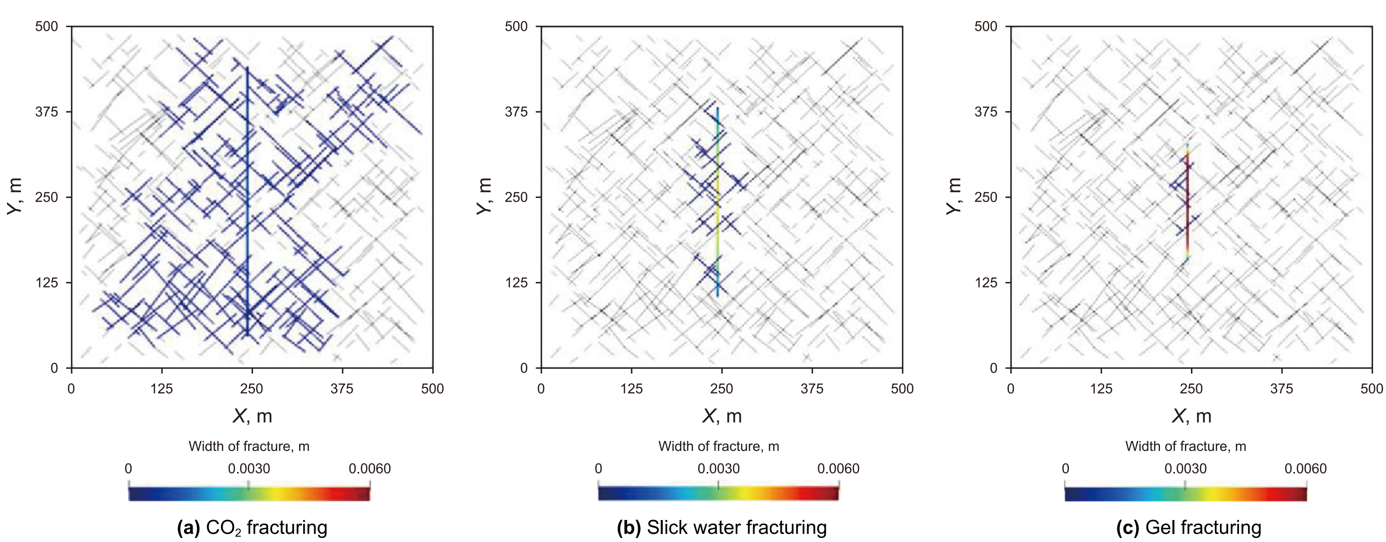

Fig. 5. Volume of active natural fractures of each fracturing fluid in single fracturing (Zhao et al., 2021).

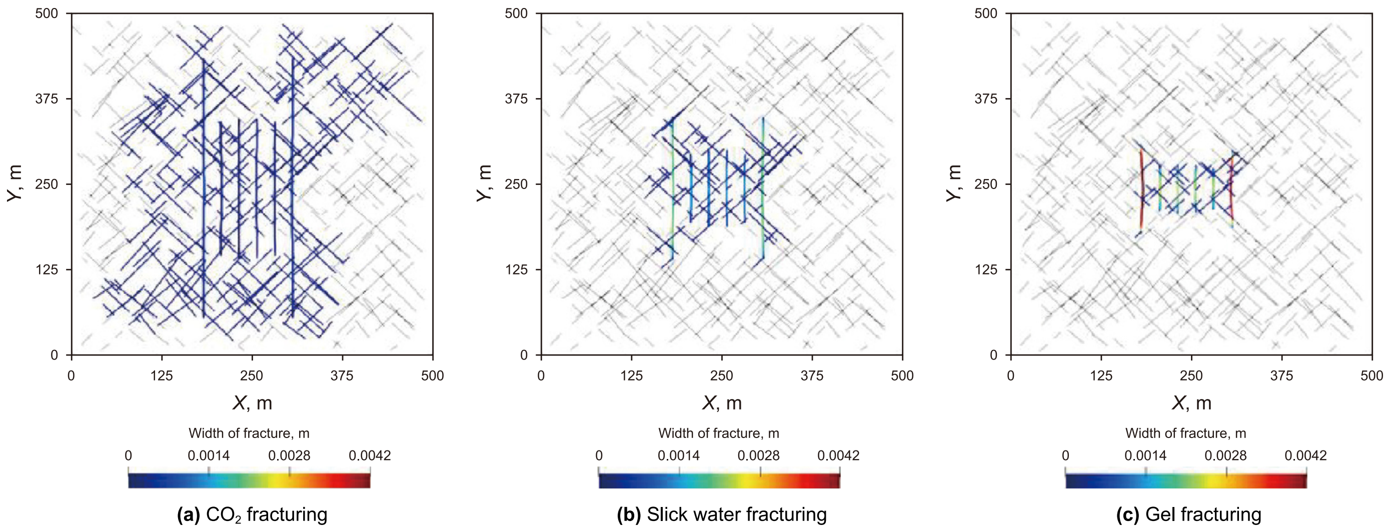

Fig. 6. Volume of active natural fractures of each fracturing fluid after multiple fracturing (Zhao et al., 2021).

the curvature of the fractures increases, as shown in Fig. 8. This indicates that more thin and narrow fractures will be generated under high temperature conditions. Furthermore, temperature has a significant effect on the morphology of induced fractures (W. Zhang et al., 2021). The fracture morphology can be divided into single fracture extending obliquely or along the direction of principal stress and fracture network formed with the increase of temperature. Liang and Li et al. analyzed the reasons for the formation of fracture networks after SC-CO_2 entered shale reservoirs (X.J. Li et al., 2018; Liang et al., 2022). It was pointed out that the Joule-Thomson effect led to a sharp drop in fluid temperature when SC-CO_2 enters the fracture, forming a temperature difference. This promotes the phase transition of SC-CO_2, accelerates the growth of fractures, which promotes the formation of complex fracture networks. Yan et al. (2021) numerically simulated SC-CO_2 fracturing in a staged manner, and observed the fracture morphology of SC-CO_2 fracturing fluid at different temperatures under the same pore pressure. With the increase of fluid temperature, the fracture length also increases.

Pressure is one of the main factors that cause rock fracture and fracture propagation. Because CO_2 molecules are easier to penetrate into rock pores, making pore pressure increases, which promotes the fracture initiation process. Liu et al. (2020) used the new numerical model to couple the unsteady flow model based on pore scale network method and the solid model based on cohesive zone element finite element method. It was found that the fracture caused by SC-CO_2 fracturing was more complicated than that caused by hydraulic fracturing (Liu et al., 2020). Fig. 9 shows the pore pressure and fracture propagation distribution of hydraulic fracturing and SC-CO_2 fracturing. The complexity of fractures is mainly showed in more branched fractures and non-expansive shear failure fractures. Compared with hydraulic fracturing, the fracture network of SC-CO_2 fracturing is more complicated, because SC-CO_2 fracturing fluid has low viscosity, miscibility with reservoir hydrocarbons and low capillary force. SC-CO_2 can penetrate into the matrix from pores, and the pore pressure increases with time. The increase of pore pressure will increase the probability of shear failure and mixed failure, and form a complex fracture network (Cai et al., 2021; Peng et al., 2017). Moreover, pressure has a significant effect on shale permeability. Liu et al. (2024) conducted true triaxial experiments on shale samples. It was observed that when the gas pressure was 3–5 MPa, the permeability increased with the increase of pore pressure. Wang et al. (2024) studied the pore throat structure of shale under high pressure by SC-CO_2, and the experimental results were consistent with those obtained by Liu et al. Shale permeability increases monotonically with the increase of CO_2 pressure, and the overall increase range was 0.4–0.6 mD. When the permeability of shale increases, under the action of SC-CO_2, the microscopic pores and fracture networks in the rock will become more connected and extensive. This means that there are more low-resistance paths, so that fracturing fluid can spread quickly and promote the formation of fractures.

Temperature and pressure are the key operating parameters in regulating the SC-CO_2 fracturing process. By changing the physical and chemical properties of SC-CO_2, they change the mechanical properties of rocks (Daniel, 2009; Ozdemir and Schroeder, 2009; Sparks et al., 2008), which in turn affects the overall fracturing effect and reservoir reconstruction. In the meantime, the decrease of effective stress caused by thermal stress and pore pressure is the main potential mechanism of fracture pressure reduction and fracture network formation in SC-CO_2 fracturing. Furthermore, it is of great significance to clarify the phase change of CO_2 fracturing fluid through temperature-pressure coupling for the initiation and propagation of fractures in shale.

2.2.5. CO_2 concentration and injection rate

Both SC-CO_2 concentration and injection rate will affect the fracturing initiation and fracture propagation in shale. The increase of SC-CO_2 concentration can increase the dissolution ability of fracturing fluid, thus enhancing the corrosion of liquid to shale rock and promoting the fracture of rock. Higher concentration of SC-CO_2 can increase the pore pressure in shale, thus promoting the formation and expansion of fractures. Increasing the injection rate of fracturing fluid can increase the possibility of fracture formation. It is helpful to form more fractures through rapid pressurization and fluid energy concentration (Hou et al., 2020). J.T. Wang et al. (2018) established a phase control model of SC-CO_2 fracturing with temperature control, and found that the change of injection rate will affect the pressure loss and fracture length expansion in the wellbore. With the increase of pumping rate, the fluid friction pressure loss increases. When the pumping rates were 2, 3, 4, 5 and 6 m^3/min, the corresponding fracture propagation lengths were 29, 42, 56, 71 and 85 m, respectively. High injection rate not only promotes the formation of complex fracture networks, but also contributes to

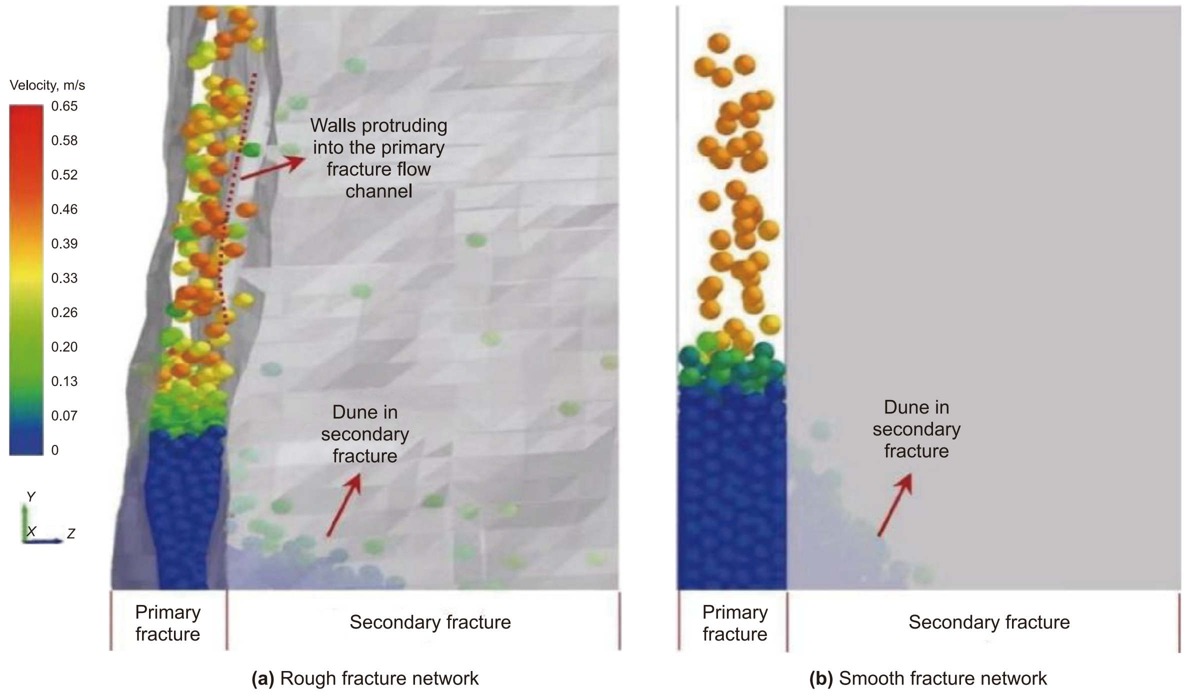

Fig. 7. Comparison of flow channel shape characteristics at the entrance of branch fractures in the two fracture networks (Zheng et al., 2024).

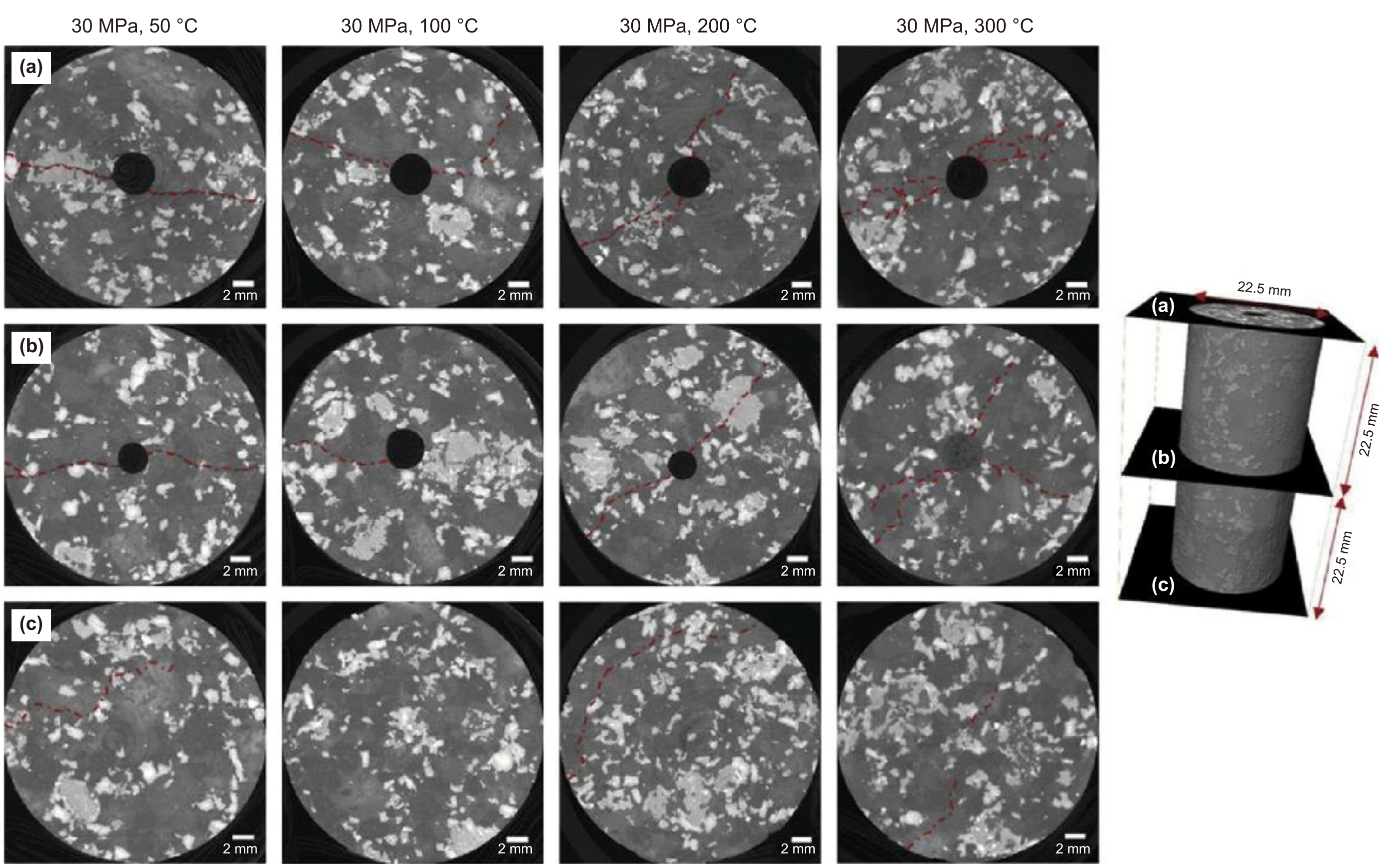

Fig. 8. CT images of different positions of SC-CO_2 crushed rock samples at different temperatures under 30 MPa confining pressure (Isaka et al., 2019).

the diffusion of proppants, which increase the possibility of rock fracture. Y. Zhou et al. (2020) established a SC-CO_2 fracturing temperature field calculation model and a three-dimensional fracture model. It was found that when the injection rate increased, the SC-CO_2 density in the fracture increased. High density will reduce the settlement of particles in fractures, which is conducive to the extension of "proppant bed". Similarly, J.T. Wang et al. (2019) established a two-phase flow model of SC-CO_2 fracturing fluid carrying proppant in fractures under unsteady state. The pumping rate of SC-CO_2 fracturing fluid was calculated, as shown in Fig. 10. It was considered that the pumping speed of SC-CO_2 fracturing fluid was 5–6 m^3/min, which can meet the transportation demand of proppant in fracturing. Because the high pumping rate corresponds to the high Reynolds number and the degree of turbulence, some proppants are converted from the surface of the embankment to the suspended layer. It increases the thickness of the suspension layer and achieves the purpose of efficient transportation of proppant. The above shows that the problem of proppant transport caused by insufficient fracture width can be alleviated by increasing the injection rate, and the fracturing effect can be further improved (Y.T. He et al., 2020).

Although the larger injection rate will improve the fracturing effect, it will reduce the rate of CO_2 heating in the fracture. When the filtration of SC-CO_2 is small or controllable, the injection rate should be as small as possible to ensure that SC-CO_2 reaches the supercritical state at a faster rate in the fracture. Thus, it is necessary to select a reasonable SC-CO_2 concentration and injection rate for different shale reservoirs to obtain the best fracturing effect.

3. Optimization of supercritical CO_2 fracturing efficiency

In practical application, SC-CO_2 fracturing is a complex process, which is influenced by many factors such as the complexity of shale reservoir. In order to further improve the fracturing effect and production efficiency, it is necessary to constantly explore innovative methods and technologies. During the fracturing operation, the fracturing efficiency and the fracturing technology can be improved by reducing the initiation pressure, expanding the fracture, optimizing the thickener and proppant, so as to promote its application efficiency and economic benefits.

3.1. Reduction of fracture pressure and propagation of fractures

The initiation pressure is to overcome the compressive strength of the rock and create fractures so that the rock can be effectively fractured, which can enhance productivity. In the process of SC-CO_2 fracturing, reducing the initiation pressure and expanding fractures are the key factors to improve the efficiency of SC-CO_2 fracturing. It can more easily realize the fracturing and expansion of rock layers or fractures, and improve the effect and productivity of SC-CO_2 fracturing. Li et al. (2019b) designed a new intermittent CO_2-hybrid fracturing method. The pure CO_2 was pumped to form a fracture network. The shale rock was soaked to promote the interaction of CO_2-salt water-rock, and finally CO_2 slurry was injected to extend the fracture. The fracturing method makes full use of the physical-chemical effect of CO_2 to improve the fracturing efficiency. Compared with SC-CO_2 fracturing, the initiation pressure of intermittent CO_2-hybrid fracturing was reduced by 21.6%, and the complexity of the fracture network formed was higher than that of SC-CO_2 fracturing, as shown in Fig. 11. In the process of CO_2 fracturing, in addition to the physical properties of CO_2, other mixtures can be added to achieve the purpose of reducing the initiation pressure and expanding the fractures. Xu (2023) established a uniaxial compressive damage constitutive model of shale under the action of N_2/SC-CO_2 gas mixture. It was found that the physical and chemical effects of N_2/SC-CO_2 mixture on shale will lead to changes in its mechanical properties. After the action of mixed gas, the tensile strength, uniaxial compressive strength and elastic modulus of shale decrease, and Poisson's ratio increases. In addition, when the concentration of mixed gas reaches the optimum ratio, it shows stronger ability of extracting organic minerals and dissolving inorganic salts, which leads to more heterogeneous distribution of

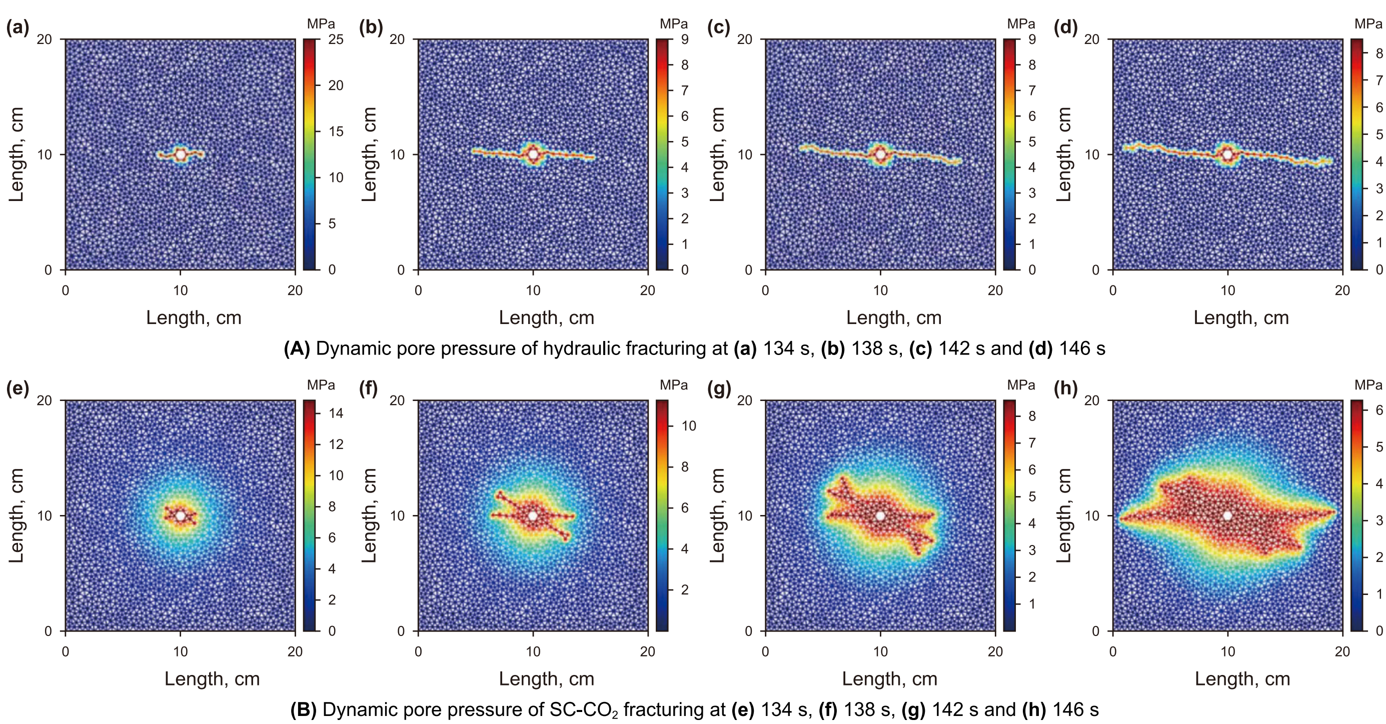

Fig. 9. Dynamic pore pressure distribution of hydraulic fracturing and SC-CO_2 fracturing. 's' is the unit of time 'seconds' (Liu et al., 2020).

pore structure in shale, thus reducing fracturing pressure and expanding fractures. Qian et al. (2023) used Pen-Robinson formula to describe the change of physical parameters of CO_2. Combined with experimental and numerical simulation methods, a simulation method of fracture propagation based on node connection method was proposed. It was found that the pre-CO_2 injection ratio had a significant effect on the branch fracture density. When the ratio of CO_2 to water increased from 0.1 to 0.3, the branch fracture density increased by 117%, which promoted fracture propagation and improved fracturing efficiency. In 2017, the field test of SC-CO_2 fracturing was carried out in Yanchang Oilfield. During the construction process, an 8.89 cm tubing was used for jetting, and a 13.97 cm casing was used for fluid replenishment. A total of 386 m^3 of liquid CO_2 was injected by using the way of oil sleeve injection at the same time. The frictional resistance and wellbore temperature profile of SC-CO_2 were tested on site, and its sand carrying capacity was tested. The sand carrying performance test used low-density ceramsite with a bulk density of 1.45 g/cm^3, and the volume fraction of ceramsite in the sand carrying liquid was about 3%. The monitoring results showed that the fracture initiation signals formed by SC-CO_2 fracturing in all directions around the wellbore were radial and evenly distributed, while the fracture initiation signals of conventional hydraulic fracturing were mainly distributed along the direction of the maximum horizontal principal stress. It shows that SC-CO_2 fracturing can break through the limitation of in-situ stress and form fractures in all directions around the wellbore. The production test results indicated that compared with the hydraulic fracturing of adjacent wells, the production increase of SC-CO_2 fracturing was more than 50%, which proved that this method can simultaneously achieve reservoir reconstruction, production increase and geological storage of CO_2 in shale gas wells. According to Fig. 12, CO_2 concentration of produced gas after fracturing about Yan-2011 well is less than 2% in the field, amounts to the concentration of CO_2 in the primary shale gas, which proves that the injected CO_2 can be effectively storaged. In addition, Hou et al. compared the field test of CO_2 huff and puff with supercritical CO_2 fracturing, as shown in Fig. 13. It was found that the recovery rate of CO_2 after fracturing in Yan-2011 well of Yanchang Oilfield was obviously lower than that after huff and puff in Hw-1003 well of Bunn camp in Tennessee, which indicated that CO_2 fracturing technology was more efficient in storing CO_2 (L. Hou et al., 2024).

The optimized fracturing method can significantly improve the fracturing effect of SC-CO_2. In the fracturing process, the dynamic damage energy required for shale to withstand external loads increases, resulting in a decrease in its brittleness index and elastic modulus. This makes the energy accumulation and release of shale tend to decrease during fracture failure, increasing the possibility of deformation. Moreover, the shale soaked in CO_2 fracturing fluid shows a tensile-shear mixed micro-fracture failure mode, in which the tensile fracture plays a leading role. This leads to a significant deterioration of the mechanical properties of shale and promotes the formation of complex fracture networks and multi-point initiation.

3.2. Optimization of thickener

Although the low viscosity of SC-CO_2 makes it easier to penetrate into rock pores, this characteristic also causes problems. For example, the fracturing fluid cannot effectively carry solid particles and the filtration rate increases (B.F. Li et al., 2018). It leads to the loss of fracturing fluid in the formation and the deposition of solid particles, thus weakening the fracturing effect on the formation. Therefore, it is necessary to increase the viscosity of the fracturing fluid to improve the fracturing efficiency. At present, SC-CO_2 thickeners can be divided into polymers, small molecule compounds and surfactants. The initial study of polymers focused on hydrocarbon polymers. However, a large amount of cosolvents need to be added to completely dissolve them in SC-CO_2. Desimone et al. found for the first time that fluoropolymers can be dissolved in CO_2 without adding cosolvents and significantly thicken CO_2 fracturing fluid under reservoir conditions (Desimone et al., 1992). However, fluorine compounds are expensive and harmful to the environment. Therefore, siloxane polymers have become a new research direction. As a polymer, polydimethylsiloxane-vinyl acetate can be completely dissolved in SC-CO_2 without adding any cosolvent. This thickener has a strong affinity for CO_2, and the thickening effect is remarkable. It is evenly distributed after mixing with SC-CO_2. Its viscosity in SC-CO_2 increases, basically meeting the requirements of on-site sand fracturing (Fu et al., 2020). Shen et al. (2022) studied branched siloxane thickeners. Compared with polydimethylsiloxane, branched siloxane thickeners showed better thickening and proppant static suspension ability in SC-CO_2 fracturing fluid. Another strategy for thickening CO_2 is to design small molecules that form a thickening network, that is, small molecule compounds. Similar to polymers, small molecule compounds are also divided into hydrocarbons, fluorinated and siloxane compounds (Zhou et al., 2021). Among them, the most obvious thickening effect is the compound containing urea bond in siloxane. For example, the viscosity of CO_2 increases by 3–300 times under low pressure for branched benzene triurea materials (Doherty et al., 2016). These small molecule compounds improve the viscosity of SC-CO_2 fracturing fluid by establishing intermolecular interactions

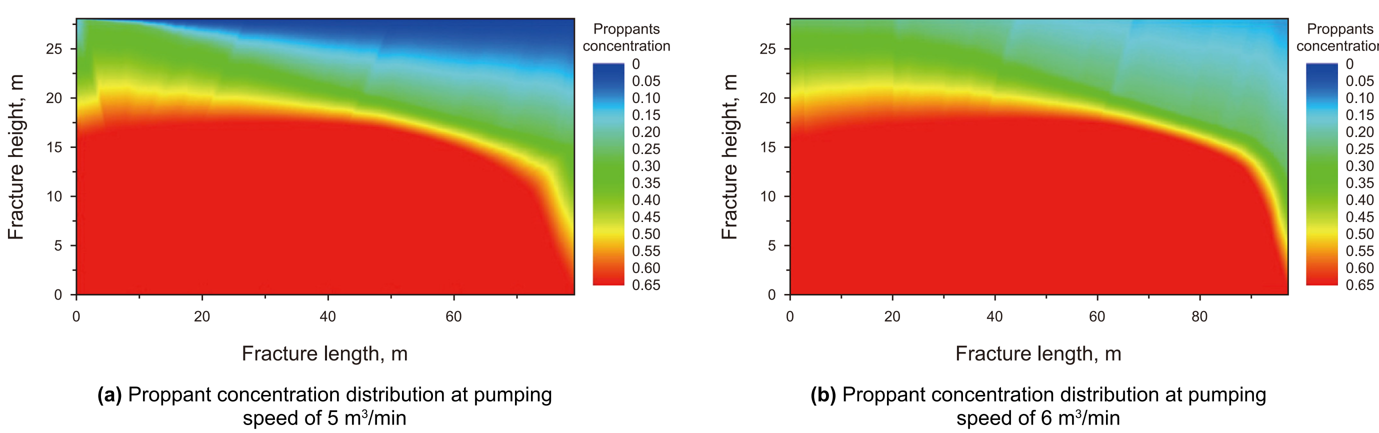

Fig. 10. Proppant concentration distribution at different injection rates (J.T. Wang et al., 2019).

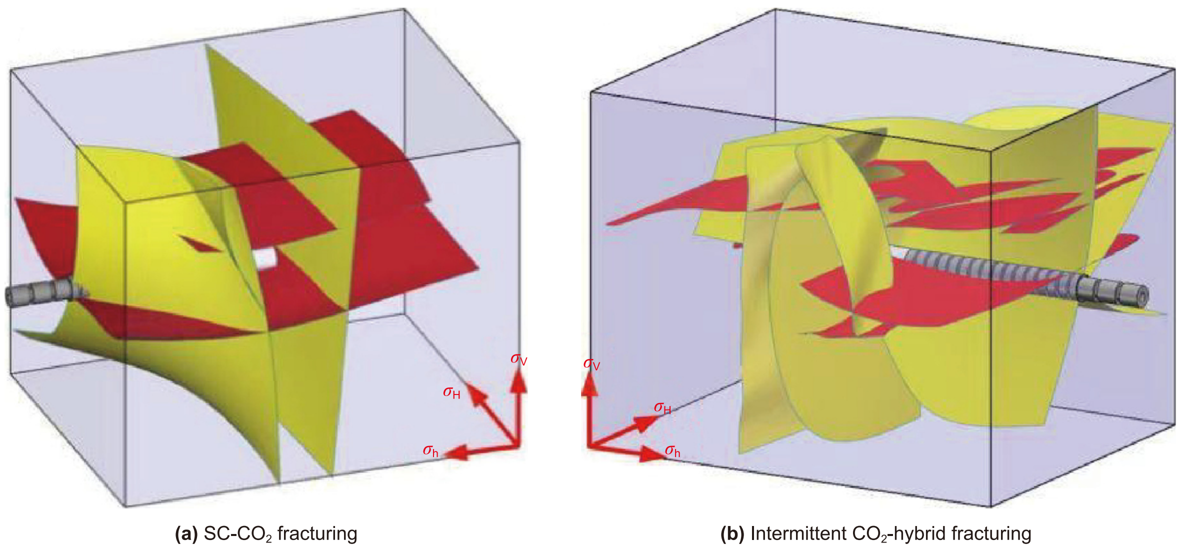

Fig. 11. Reconstruction of fracture geometry (yellow surface is HFs, red surface is BP) (Li et al., 2019b).

that increase viscosity, thereby improving the sand carrying capacity and filtration of fracturing fluid. As a clean polymer-free fracturing fluid, surfactant fracturing fluid has become the focus of current research on thickeners. It has the characteristics of no residue, little damage to the formation and good sand carrying performance (Ma et al., 2021; Zhang et al., 2013). The mechanism of action is based on the formation of layered, rod-like, worm-like and other ordered structures by the spherical micelle structure of the surfactant under the action of the counter-ionic salt, thereby improving the consistency and rheological properties of the SC-CO_2 fracturing fluid (Hou et al., 2023). The surfactant also significantly improves the temperature resistance of the fracturing fluid while increasing the viscosity. J. Zhao et al. (2018) synthesized a trimeric cationic surfactant containing erucic acid group. It was found that the system formed by the purified trimeric cationic surfactant and the counter ion salt sodium salicylate had a temperature resistance of 180 °C.

In recent years, researchers have begun to explore the application of nanomaterials in fracturing fluid thickeners. Nanomaterials have a good synergistic effect on SC-CO_2 thickening system due to their small particle size and strong surface effect, which significantly improves its thickening, temperature resistance and sand carrying capacity (Wang et al., 2022). W.L. Qin et al. (2017) added 0.3%(w) polyhydroxy carbon nanotubes to the system containing 3%(w) polyamidopropyl betaine, and the temperature resistance of the system was improved from 110 to 130 °C. S.C. Liu et al. (2022) prepared a novel silica nanoparticle-enhanced CO_2-sensitive fracturing fluid system. The sedimentation rate of CO_2 sensitive fracturing fluid system was reduced by 23.1%. It is proved that silica nanoparticles can improve the sand carrying capacity and reduce the filtration of CO_2 sensitive fracturing fluid.

With the in-depth understanding of the thickening mechanism, researchers found that compounds soluble in CO_2 have specific physical properties, such as low cohesive energy density, high free volume, low solubility parameters and Lewis acid-base groups. Thickener molecules can enhance their interaction with SC-CO_2 by introducing CO_2-philic groups. The CO_2-phobic moieties that are intended to associate with the other adjacent CO_2-phobic moieties, thereby establishing a viscosity-enhancing, associating network. In addition, the preparation of high-efficiency, environmentally-friendly and cost-controllable thickener has broad prospects by establishing the molecular model of nanoparticle-CO_2 system. Optimizing thickener can effectively prevent fracture closure or sand blockage, and maintain the long-term role of fracturing fluid in fractures. It is helpful to the stable extension of fractures, thus improving the durability of fracturing effect.

3.3. Proppant optimization

A certain proportion of proppants should be injected in fracturing operation to improve fracture stability and gas productivity. The low viscosity of SC-CO_2 leads to low proppant carrying capacity, which limits the proppant from entering the formed fractures, thus reducing the conductivity of the fractures (Du et al., 2018). The settling speed of proppant in SC-CO_2 is relatively high. The balanced proppant dike is formed at the bottom of fractures around the fracturing well, which makes most fracturing fractures and almost all secondary fractures unsupported (Zheng et al., 2020). Therefore, the optimization of proppant is of great significance for improving the fracturing efficiency of SC-CO_2 in shale oil and gas exploration.

Proppants can be filled in fractures, which can enhance the supporting ability of fractures and prevent them from closing in the production process. This is conducive to enhancing the permeability of fractures and productivity of oil well. At present, the most studied proppant types mainly include fracturing sand, ceramsite, resin coated proppants and so on. Fracturing sand can be carefully screened and classified to form suitable shape and size, which is helpful to resist the closure pressure of overburden. Under high shut-in pressure, sand bodies are relatively easy to form fine particles, so they are more suitable for use at a depth of about 4000 feet (Pangilinan et al., 2016). However, performance may drop drastically under closure pressures exceeding 10000 psi. As a substitute for fracturing sand, ceramic proppant has better performance under higher sealing pressure. The ceramic proppant is made of bauxite and kaolinite clay as raw materials and sintered at high temperature. Its strength increases with the increase of density, which means that the higher the alumina content, the better the mechanical properties. Ceramic proppants are classified by their density as the high-density ceramics (HDC), intermediate density ceramics (IDC), and lightweight density ceramic proppants (LDC) (Saldungaray and Palisch, 2013). LDC has high compressive strength, which is suitable for shallow reservoirs with a shut-off pressure of about 7000 psi, and can enhance fracture conductivity and obtain better fracturing effect. The specific gravity of IDC is

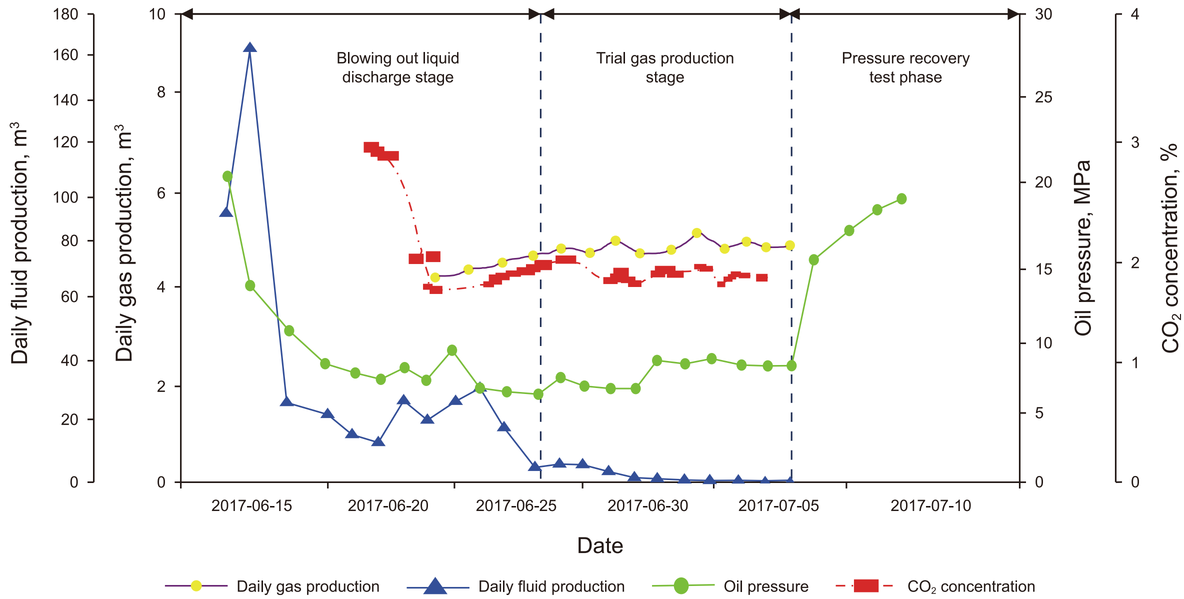

Fig. 12. Production test curve of SC-CO_2 fracturing field test in Yan-2011 well of Yanchang Oilfield (Lu et al., 2021).

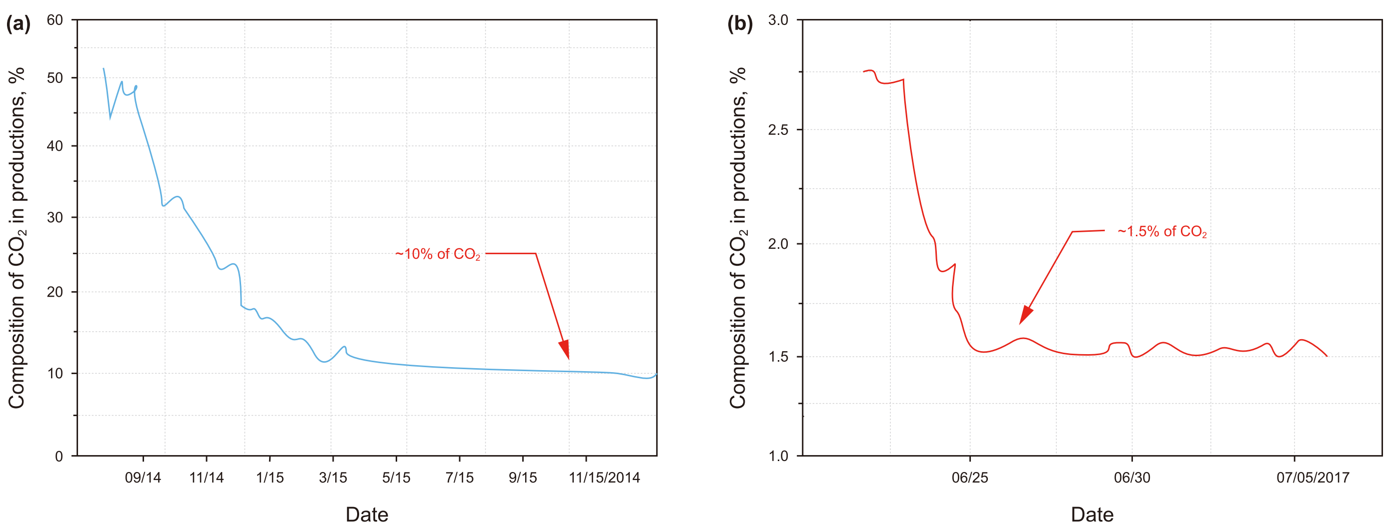

Fig. 13. Recovery rate of CO_2 after field test. **(a)** Hw-1003 well (CO_2 huff and puff field test) (Louk et al., 2017), **(b)** Yan-2011 well (SC-CO_2 fracturing field test) (Lu et al., 2021).

between 3.1 and 3.3 g/cc, which is suitable for deep wells with overburden pressure of 10000 psi. HDC is used in 14000 psi deep water and extremely high shut-off pressure area (Danso et al., 2021). Resin coating improves the tolerance of proppant in acidic environment. Therefore, resin coated proppants can maintain long-term fracture permeability and improve fracture conductivity by protecting proppant from the influence of closure stress and formation temperature (Goldstein and VanZeeland, 2015; Nguyen et al., 1998). There may be two forms of resin coated proppants, one is pre-cured or partially cured at the manufacturing site, and the other is a liquid resin that is in-situ cured on the surface of the proppant in response to temperature and closure pressure in the formation (Vo et al., 2014). Bandara et al. compared the porosity produced by sand mold, ceramic and resin coated proppants (Bandara et al., 2021). The proportion of fine particles produced by fracturing sand, ceramic and resin coated proppant was 51%, 35% and 6% respectively. After loading cycle, the porosity decreased by 98%, 88% and 75% respectively.

Recent studies have proved that smaller submicron or nano-proppants can improve the oil recovery of unconventional shale reservoirs. Traditional proppants cannot invade the tiny fracture aperture and rough fracture surface. When the hydraulic pressure is removed, the fracture will close again, and forming a blind spot and reducing the effective fracturing volume. Therefore, using smaller proppants cannot only support them to open, but also make up for the diversion loss caused by thinner propping fractures, and promote the long-term production of shale gas (C.P. Zhang et al., 2021). The negative correlation between fracture aperture and matrix permeability also promotes the application of smaller proppants in shale gas formations (L. Wang et al., 2018). In addition, the concentration and size of proppant have significant influence on fracture propagation. According to the proppant concentration, the fracture morphology can be divided into four areas: low area, suspended area, tumbling area and proppant reservoir area. Among them, proppant reservoir area and suspension area are two key areas that affect fracture morphology (Song et al., 2018). Zheng et al. compared the two ways about proppant step-up concentration and step-decreasing concentration (Zheng et al., 2022b). It was concluded that the velocity of fluid on the surface of proppant was proportional to the concentration of injected proppant. It was also found that a longer diffusion distance of proppant can be obtained by decreasing the concentration of injected proppant step by step. The size of proppant is also crucial to fracture propagation. As observed from the simulation results in Fig. 14, compared with 40/70 mesh and 20/40 mesh proppants, 200 mesh and 100 mesh proppants have slower sinking speed, more uniform distribution and larger effective support area. It shows that finer proppant can be distributed more effectively in complex fracture network (Kumar et al., 2019).

Proppant plays an important role in SC-CO_2 fracturing. Optimizing proppant can effectively fill the fracture gap, and provide more supporting force, which prevent the fracture from closing or decreasing rapidly. In the fracturing operation of plateau stress, the ceramic proppant with large size and high concentration can maintain high filling porosity. In order to reduce the embedding depth of proppant, it is recommended to use resin coated proppant instead of ceramic or sand proppant. Furthermore, it is suggested that proppant with smaller size and higher concentration should be selected in sedimentary strata and low stress depth stimulation projects. The newly researched nano-proppants not only make up the conductivity loss of propping fractures, but also increase the flow distance of proppants in fracture channels. The effective width and length of fractures are further increased, which maintain a good seepage channel. This is conducive to the smooth outflow of oil and gas and improve oil recovery.

4. New technology of supercritical CO_2 fracturing

Experimental research shows that the fracture induced by SC-CO_2 fracturing is narrow, which is not conducive to the entry of proppant and gas transport (Li et al., 2019a). Due to the low viscosity of SC-CO_2, the bearing capacity of proppant is weak, and the fracture is easy to close after fracturing, which leads to the decrease of fracture conductivity. Therefore, researchers put forward a new technology about SC-CO_2 fracturing. The appearance of new technology provides more choices for fracture propagation in shale. They cannot only improve the effect of fracture propagation, but also reduce the demand for water resources and reduce the impact on the environment. Although these technologies still have some challenges such as technical maturity and economic feasibility, they provide new possibilities for shale development.

4.1. Supercritical CO_2 jet fracturing technology

SC-CO_2 jet fracturing is a technology of rock fracture using CO_2 jet in supercritical state. Firstly, CO_2 is pressurized to supercritical state, and the SC-CO_2 jet is injected at high pressure, which directly acts on the rock layer, causing the rock to fracture and form tiny fractures. The natural gas or oil reservoir in the reservoir is released. In previous studies, hydraulic jet fracturing is a unique and efficient fracturing technology, which can successfully complete multi-stage fracturing without a large number of mechanical packers (Surjaatmadja et al., 1998). SC-CO_2 jet fracturing combines the advantages of hydraulic jet fracturing and SC-CO_2 fracturing. The temperature and heat transfer distribution of SC-CO_2 jet fracturing in perforated tunnel is different from that of water jet, which has a positive impact on the initiation and propagation of fractures (Cai et al., 2017; Hu et al., 2016).

SC-CO_2 jet fracturing technology has its unique advantages in the formation and connection of rock fractures. Supercharging of SC-CO_2 jet in perforation easily leads to the initiation and propagation of fractures, thus increasing the distribution range and number of fractures (Cai et al., 2018). He et al. deeply studied the pressurization mechanism of SC-CO_2 jet in the perforation process, and conducted experimental research (He et al., 2015). The effects of pressure difference, ambient pressure, fluid temperature and nozzle diameter were discussed. Hu et al. used numerical simulation based on fluid-solid coupling and user-defined code to study fracture initiation in heterogeneous shale (Hu et al., 2017). It was found that the high-speed jet of SC-CO_2 increased the stress of shale and led to the fracture initiation at the perforation position. As the diameter of the nozzle outlet and the perforation pressure increase, more fractures appear at the tip. With the increase of aspect ratio and aperture ratio, the initial position of fracture propagation extends. Based on SC-CO_2 jet fracturing, it was considered that the pre-breakdown of cyclic injection may lead to the decrease of breakdown pressure and the increase of stimulated layer (Erarslan and Williams, 2012; Patel et al., 2017). Cai et al. combined the advantages of pulse jet and multiple fracturing, and put forward the experiment of enhanced jet fracturing with multiple pulse SC-CO_2 jet (Cai et al., 2019). Multi-pulse SC-CO_2 jet fracturing was a process of strong impact and pressurization, and the cumulative residual strain was used to promote the initiation and propagation of fractures, making the fracture network more complicated. It was observed that with the increase of pulse jet frequency and jet pressure, the number and curvature of fractures increased. Fig. 15 shows that compared with pulsed water jet fracturing, pulsed SC-CO_2 jet fracturing can produce more complex fracture morphology and larger fracture volume. Subsequently, Cai et al. established the induced strain model, and made a comprehensive study on the fracture generation and strain change in the process of SC-CO_2 jet fracturing (Cai et al., 2022). It was found that with the increase of jet pressure, a large number of fracture branches were formed, and the main fracture mode changed from curved double-wing fracture to multi-fracture. Environmental pressure will affect the propagation path of fractures. The number of fractures under different jet distances was summarized, and the results were similar to the previous research data, indicating that the optimal jet distance can play a positive role in jet fracturing.

SC-CO_2 jet fracturing technology uses the characteristics of fluid density and viscosity to improve jet velocity and reduce friction resistance, thus increasing the energy conversion efficiency from motion state to static state. Supercharge of SC-CO_2 jet caused by kinetic energy conversion of jet significantly increases perforation pressure, making it easier for fractures to start-up and expand. Under the same conditions, the viscosity of SC-CO_2 is one order of magnitude lower than that of water. It has stronger permeability and is easier to continue to expand to micro-pores, micro-fractures and other damage, which increases the scope of jet action and strengthens the rock breaking effect (Du et al., 2019). For example, Kolle and Marvin found that under the injection pressure of 55~193 MPa, the pressure of SC-CO_2 jet breaking rock was 2/3 of the pressure of water jet breaking rock in marble samples, and 1/2 or less of the pressure of water jet breaking rock in shale (Kolle and Marvin, 2000). Li et al. studied the mechanism and method of SC-CO_2 jet fracturing. It was found that the pressure in the pore of SC-CO_2 jet was higher than that of water jet under the same conditions. It shows that SC-CO_2 jet fracturing has a stronger jet pressurization effect than water jet, which is beneficial to open the formation under lower annular pressure (G. Li et al., 2013).

In summary, under conventional formation and operating conditions, the pressurization effect of SC-CO_2 jet fracturing in the perforation channel can be close to or even exceed that of water jet fracturing. In deep well operations, with the increase of pressure and temperature in unconventional reservoir environment, SC-CO_2 is expected to provide more effective pressure effect. It is more

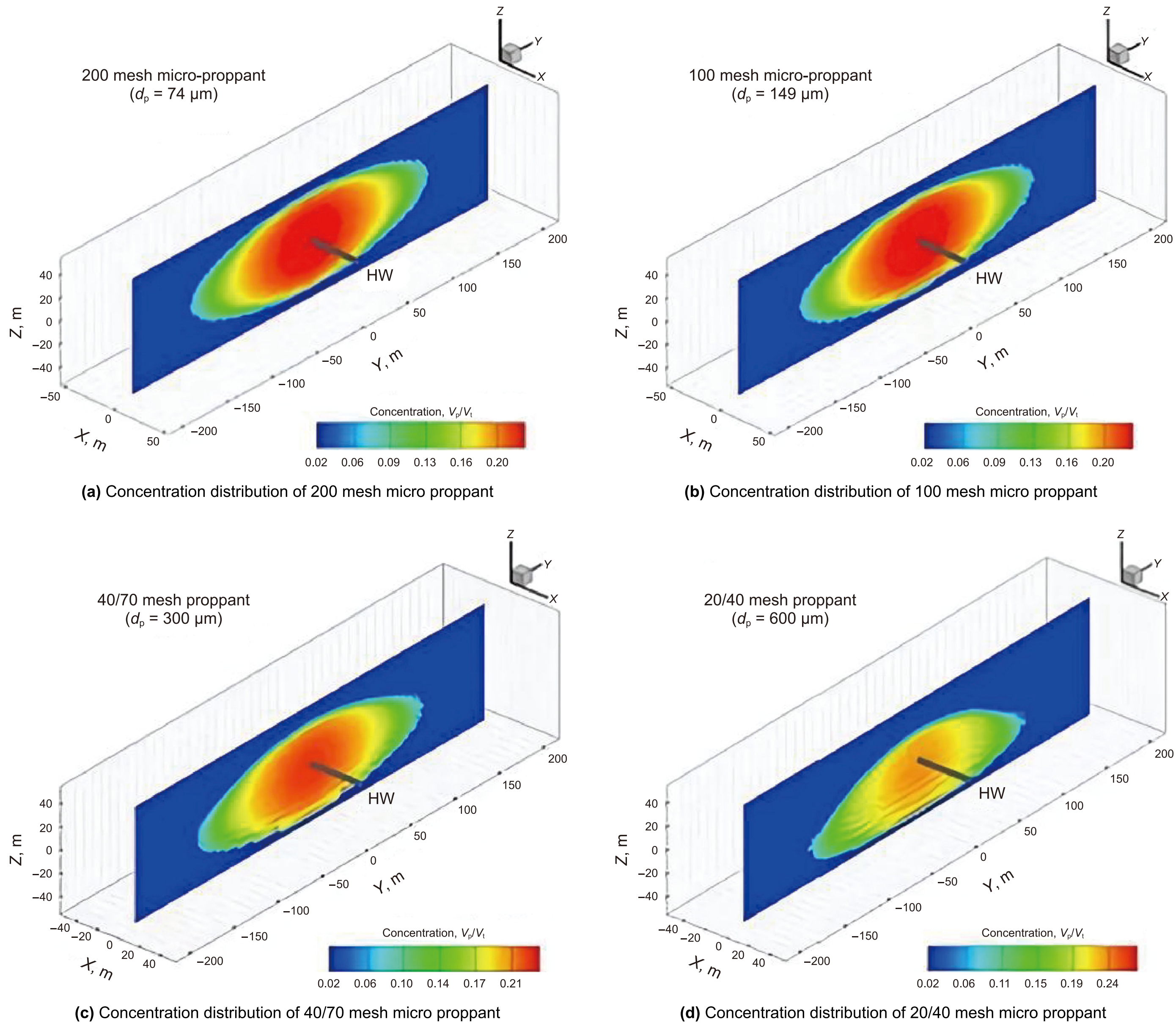

(a) Concentration distribution of 200 mesh micro proppant

(b) Concentration distribution of 100 mesh micro proppant

(c) Concentration distribution of 40/70 mesh micro proppant

(d) Concentration distribution of 20/40 mesh micro proppant

Fig. 14. Micro proppant concentration distribution (C.P. Zhang et al., 2021).

suitable for unconventional reservoirs than other conventional fluids. However, not all geological conditions are suitable for SC-CO_2 jet fracturing, because the physical and chemical properties of the formation may lead to uneven response. For example, there may be significant differences in the degree of fracture propagation and oil and gas recovery in different regions. At present, SC-CO_2 jet fracturing technology is still in the research and development stage, and related technologies and equipment are not yet mature. Most of the jet fracturing experiments are mainly based on homogeneous rocks, without fully considering the actual situation of shale reservoirs. There is also a lack of in-depth theoretical research and quantitative analysis on the specific situation of SC-CO_2 jet enhanced fracturing effect. Therefore, it is necessary to fully consider the influence of different shale characteristics and reservoir heterogeneity on fracturing effect in order to analyze fracture propagation more accurately in real reservoirs, so as to speed up the field test process of SC-CO_2 jet fracturing technology.

4.2. Supercritical CO_2 compound fracturing technology

SC-CO_2 compound fracturing technology is a new technology combining SC-CO_2 with other fracturing fluids. That is, SC-CO_2 is used as cushion fluid to generate fracture network, and then water-based fluid is used as carrier fluid to widen and support the network, so as to achieve higher fracturing effect and productivity. The advantage is that it can be adjusted and optimized according to different geological conditions and production requirements in combination with different fracturing fluids, thus improving fracturing effect and productivity.

Aiming at the key technical problems of volume fracturing of heterogeneous continental shale reservoirs with high clay mineral content, Liu et al. put forward the SC-CO_2-hydraulic compound volume fracturing technology and successfully applied it in practice (W.B. Liu et al., 2022). Firstly, SC-CO_2 pre-fracturing was carried out to reduce formation fracturing pressure and increase longitudinal penetration. Then, large-scale hydraulic fracturing was carried out.

The sand was carried with large displacement, which expanded the formed complex fracture network and effective support on a large scale. The experiment and field practice prove that the SC-CO_2-hydraulic compound fracturing technology has a remarkable effect. It can decrease the fracture initiation pressure and reservoir heterogeneity of shale reservoirs and lay a foundation for forming a complex fracture network. In the experiments of Zang et al., SC-CO_2-hydraulic compound fracturing also achieved the same effect (Zang et al., 2024). Pre-SC-CO_2 injection triggered physical and chemical reactions with rock samples, and led to a downward trend of elastic modulus and compressive strength. The failure mode was gradually changed from brittle shear failure to plastic failure. The ability of SC-CO_2 pre-fracturing to create complex fractures was much greater than that of hydraulic fracturing. The complex fracture network was rapidly formed in a short time to achieve the purpose of volume transformation. The fracture pressure of SC-CO_2-hydraulic compound fracturing was 16.6% lower than that of hydraulic fracturing. It was proved that SC-CO_2-hydraulic compound fracturing can dissolve and transform shale oil reservoirs at the micro scale, which improved the seepage capacity of shale oil reservoirs.

Facing the problem that low viscosity CO_2 can obviously restrain the fracture height, Li et al. put forward a new SC-CO_2-gel fracturing method to stimulate shale reservoirs with a large number of weak bedding planes (Li et al., 2020). Firstly, high viscosity gel was injected to initiate fractures, and then CO_2 was pumped to extend gel-induced fractures. It was found that tensile failure dominated the process of fracture formation during single-phase fracturing. Shear failure in SC-CO_2-gel fracturing dominated the formation of fractures, and shear failure was most likely to induce pre-existing natural fractures or bedding planes. Fig. 16 shows that SC-CO_2-gel fracturing may induce more fractures than single-phase fracturing using CT scanning and AE monitoring technology to measure the fracture shape. The fracture height and number produced by SC-CO_2-gel fracturing were much higher than those produced by SC-CO_2, slick water and gel single-phase fracturing. More bedding planes was activated in the horizontal direction, thus increased the volume of stimulated reservoir. In the case of SC-CO_2-gel fracturing, pre-filled or pre-pumped high viscosity gel can significantly reduce the filtration rate of SC-CO_2, which make it deep into fracture channels and induce natural fractures. It is proved that SC-CO_2-gel fracturing is feasible for increasing production of shale reservoirs with weak bedding.

Due to the poor bearing capacity of SC-CO_2 fracturing proppant

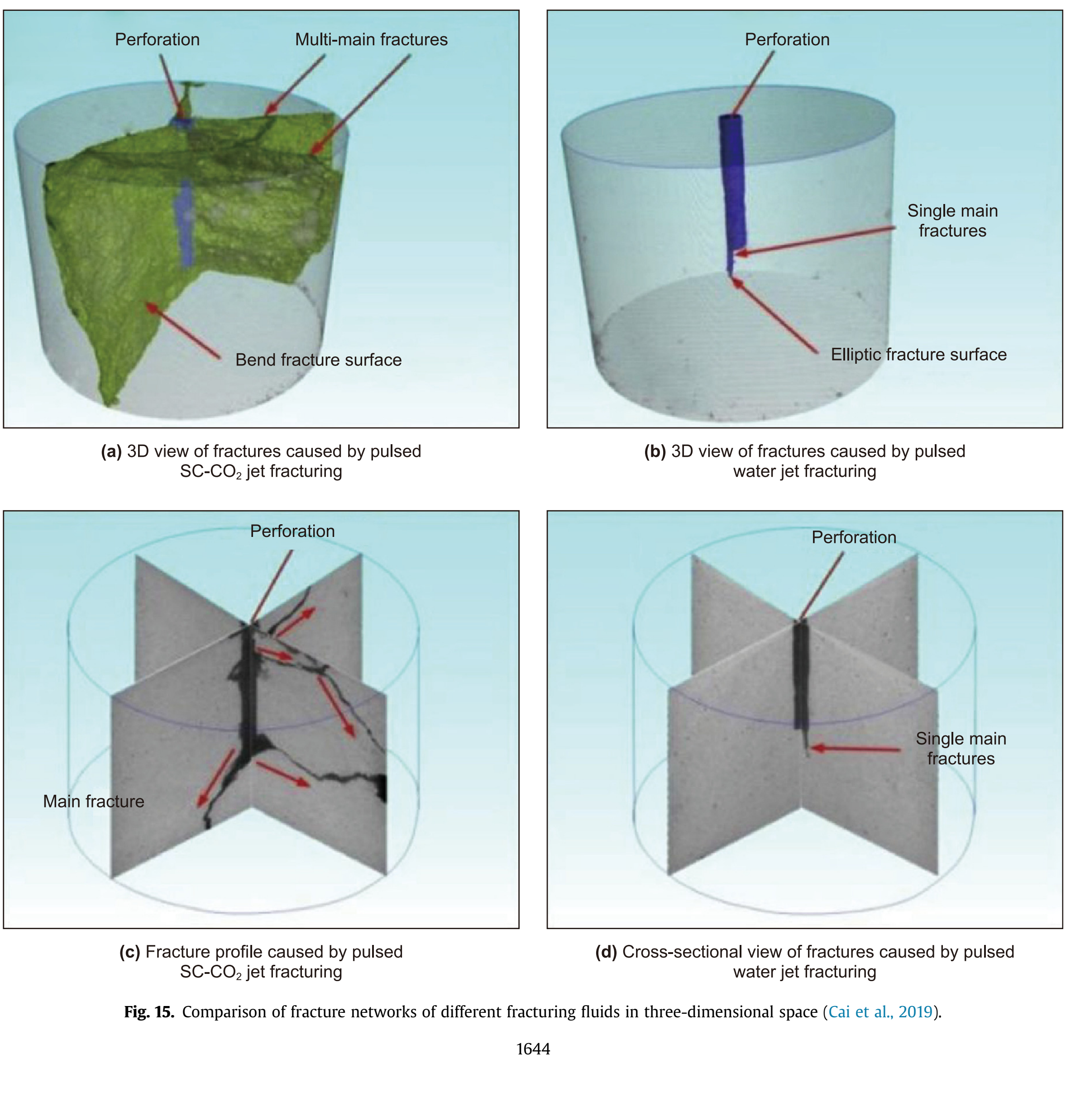

(a) 3D view of fractures caused by pulsed SC-CO_2 jet fracturing

(b) 3D view of fractures caused by pulsed water jet fracturing

(c) Fracture profile caused by pulsed SC-CO_2 jet fracturing

(d) Cross-sectional view of fractures caused by pulsed water jet fracturing

Fig. 15. Comparison of fracture networks of different fracturing fluids in three-dimensional space (Cai et al., 2019).

in shale gas development, its practical application effect is limited. Chen et al. designed the true triaxial SC-CO_2-guar compound fracturing experiment of shale (Chen et al., 2021). SC-CO_2 was used as cushion fluid to form a complex fracture network, and guar gum was used as carrier fluid to support and extend fractures. It was found that SC-CO_2-guar compound fracturing and SC-CO_2 fracturing can form more complex fracture geometry than guar fracturing. SC-CO_2-guar compound fracturing was more likely to break through the constraint of in-situ stress and connect bedding plane with natural fracture, thus forming a complex three-dimensional fracture network. Fig. 17 shows that the fracture width caused by SC-CO_2 fracturing is less than 0.01 mm, while the fracture width caused by SC-CO_2-guar gum compound fracturing can reach 0.12 mm. The width of branch fracture caused by SC-CO_2-guar gum compound fracturing is several times that of main fracture caused by SC-CO_2. It is proved that SC-CO_2-guar compound fracturing has better stimulation effect.

SC-CO_2 compound fracturing technology can improve the bearing capacity of proppant by optimizing the fracturing fluid and adjusting the injection sequence of fracturing fluid. This technology can enhance the fracture effect and form a complex fracture network. It can also significantly reduce the shale fracture pressure and improve the reservoir conditions, thus effectively improving the seepage capacity of the reservoir. Therefore, better fracturing effect can be achieved in shale and tight oil and gas reservoirs. The field test of this technology has been reported in China. For example, the first shale oil horizontal well in Songliao Basin-Jiyeyou 1HF well, it was adopted the fracturing scheme of "SC-CO_2 pre-fracturing to create complex fracture network + high-viscosity glue to make main fracture + variable viscosity slick water to effectively expand and support complex fracture network", and completed the fracturing construction of 21 sections/1431 m of horizontal wells. The volume fracturing of continental shale oil reservoirs with high clay mineral content in Songliao Basin was successfully completed. After fracturing, a high-yield industrial oil flow with an average stable yield of 16.4 m^3/d was obtained. Through CO_2 combined with gel fluid sand fracturing in Jilin Oilfield, the fracturing fluid filtration rate is reduced and the flowback rate is increased. During the fracturing process of Chengshen 131 well, the total liquid volume was 616 m^3. The total sand volume was 77 m^3. The construction pressure was 23–47 MPa, and the daily flowback volume reached 150 m^3 at the initial stage after fracturing. The cumulative flowback rate of fracturing fluid reached 50%, and the transformation effect was better than that of adjacent wells. The compound fracturing experiment was carried out in Ansai Oilfield in the middle of Ordos Basin. According to the statistical data of 46 wells, the average production of compound fracturing increased by more than 35%, and the injection of water injection wells increased by more than 50%. Then, the Dongsheng gas field in the north of Ordos also used the SC-CO_2 composite dry fracturing technology to obtain a successful pilot. The mixed composite fluid with a purity of more than 90% CO_2 fracturing fluid was used as a sand-carrying fluid. The super rock breaking ability of SC-CO_2 was used to overcome the horizontal stress difference, and entered the formation fracture, thereby generating a complex fracture network.

In fact, compared with the traditional fracturing technology, SC-CO_2 composite fracturing technology is more complex. In the fracturing process, it is necessary to further consider the composition, proportion, density, dose size, pumping rate, and completion parameters of the two fluids, thereby increasing the complexity of construction in field applications. Moreover, SC-CO_2 compound fracturing requires special equipment and technology, and the initial investment and maintenance costs are high. In addition, the technical requirements for operators are high, and the pressure and flow rate of SC-CO_2 need to be accurately controlled to ensure the fracturing effect.

4.3. Supercritical CO_2 pneumatic fracturing technology

Due to high efficiency and low cost, blasting fracturing is widely used in rock excavation related applications (Yang et al., 2016). However, blasting will produce strong shock waves, which will disturb and destroy nearby rocks and cause vibration damage to distant rocks. This will affect the stability of rocks and the safety of surrounding environment to some extent (Dowding et al., 2016; Hasanipanah et al., 2016; Sevinç et al., 2017). CO_2 phase transition fracturing is similar to blasting fracturing process, which is dynamic fracturing. In phase transition fracturing, high-pressure gas cannot cause fracture in the expansion pipe, but can only be discharged towards the end of the reservoir pipe. It has certain limitations and is easy to cause explosion and pipeline flying out. Hu et al. put forwarded a new CO_2 pneumatic fracturing technology (Hu et al., 2019). This technology used gas shock wave and static gas to release a lot of heat through rapid combustion. While ensuring safety, CO_2 copolymer is used to achieve fracturing in rocks. Compared with the traditional CO_2 phase change technology, the difference of this technology is that the excitation of chemicals only generate heat, but not release a lot of gas (Zhang and Wang, 2018; Zhu et al., 2022). This study provides a new possibility for the field of CO_2 fracturing technology in shale reservoir exploitation.

Based on this new type of CO_2 pneumatic fracturing, Wang et al. pioneered the development of a true triaxial SC-CO_2 pneumatic fracturing system. The effects of SC-CO_2 pneumatic fracturing on the initiation and propagation of induced fractures under different initial pressures and additives were studied (Wang et al., 2023). The experimental results showed that the more dosage of chemicals, the more complicated the fractures produced by the samples under the same initial pressure were. By calculating the fracture area, it was found that the fracture area increased with the increase of initial pressure under the same dosage of chemicals. The annular fracture also occurred when the rock was broken by SC-CO_2 pneumatic in the experiment. As shown in Fig. 18, the annular fracture under different pressures and agents is a tensile damage under the action of stress waves. The stress wave produce the initial fracture. The high-energy gas expand the fracture. The length and width of the fracture in the sample are increased, and the failure is finally achieved.

SC-CO_2 pneumatic fracturing technology mainly uses the impact pressure to produce initial fractures, then produces circumferential fractures and surface shedding damage under the action of stress waves. Through the action of air wedge, high-energy CO_2 fluid expands fractures. As a new type of waterless fracturing technology, it has some advantages, such as reducing water consumption and shale fracture pressure, good fracturing effect and so on. With the development of technology and practice, it has a potential prospect in the exploitation of low permeability oil and gas reservoirs and geological reservoirs with relatively high hardness. During the experiment, it was found that although the volume of energy-accumulating agent in SC-CO_2 pneumatic fracturing was relatively large, the actual energy-accumulating dose utilization rate was only 1/2. Moreover, in the energy calculation, the error of the formula derived from the gas equation is large. When the gas is at the critical point, the ideal gas state equation is no longer applicable. The equation reflecting the actual state of the gas must be used to improve the accuracy. At present, the experiment does not consider the change of gas temperature after the excitation of the energy-accumulating agent, and this parameter is very important in energy calculation and fracturing effect. In the future, temperature sensors should be introduced to monitor the

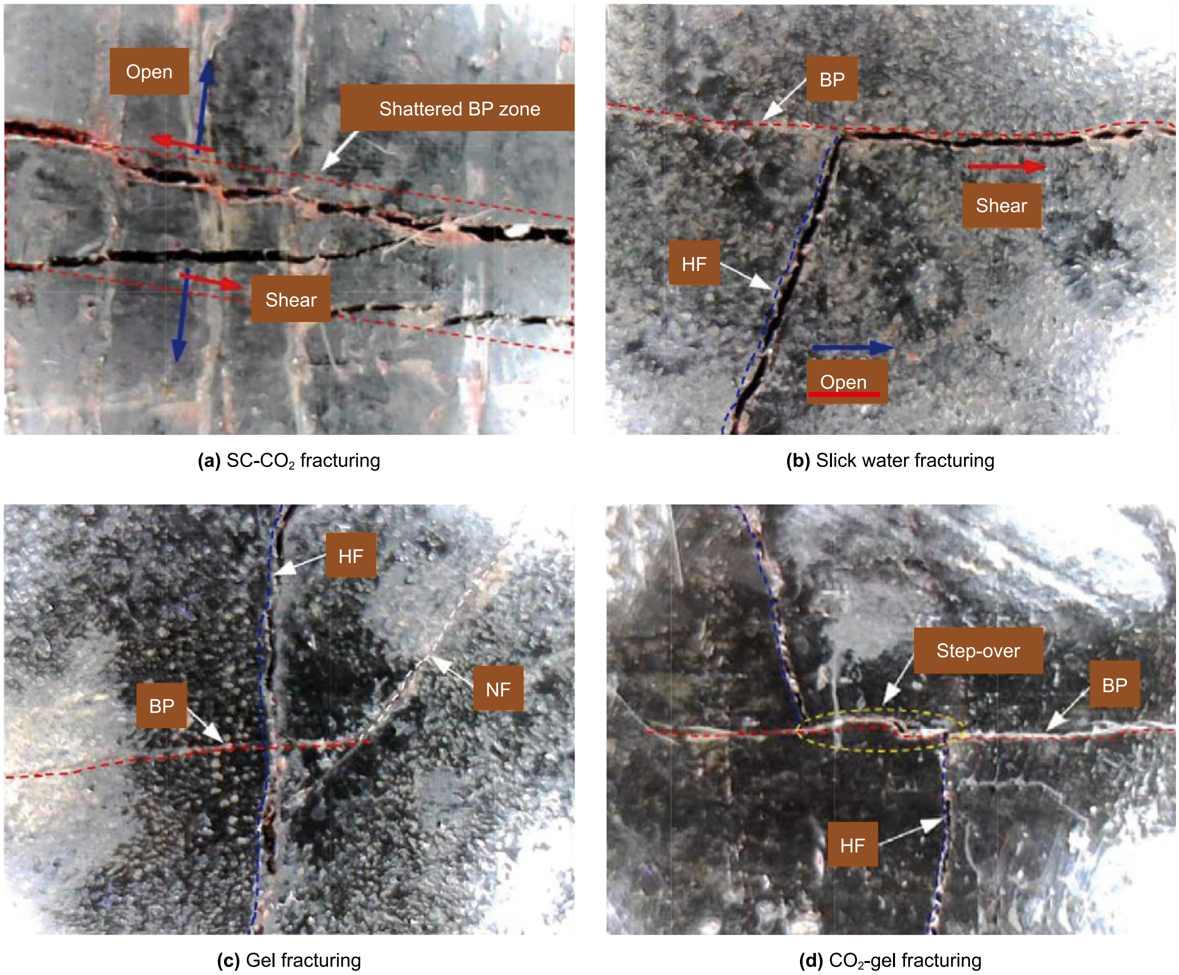

Fig. 16. Cross behavior of various hydraulic fractures (HF) and bedding planes (BP) (Li et al., 2020).

temperature change in the fracturing tube. In addition, in the SC-CO_2 pneumatic fracturing technology, it is not clear which factor plays a dominant role in the formation of rock fractures. At present, only laboratory research has been carried out. The technology is not yet mature, and it has not been tested on site. Therefore, SC-CO_2 pneumatic fracturing technology still needs further to be developed.

5. Prospects and challenges

SC-CO_2 fracturing technology is an unconventional reservoir reconstruction method that uses SC-CO_2 as a fracturing fluid to improve the permeability and conductivity of rocks. It can effectively improve oil and gas production and recovery. Compared with other fracturing technologies, the fracture pressure of SC-CO_2 fracturing shale is relatively low. The formed shale fractures have the characteristics of "large width in one-way expansion and high density in dispersed expansion". It is easier to form a complex fracture network, so as to achieve sustainable oil and gas exploitation. As a renewable resource, CO_2 can reduce the demand for water resources and decrease the impact on the environment by recycling and reusing. SC-CO_2 fracturing technology can also achieve geological storage and effectively mitigate climate change. Therefore, compared with the traditional hydraulic fracturing technology, SC-CO_2 fracturing technology has the advantages of environmental friendliness and good fracturing effect, which is in line with the trend of green development.

In the SC-CO_2 fracturing technology, the fracturing efficiency can be improved by reducing the initial fracturing pressure, expanding the fracture network, optimizing fracturing fluid and proppant. It can also be innovated and improved on the basis of fracturing technology, such as SC-CO_2 jet fracturing technology, SC-CO_2 compound fracturing technology and SC-CO_2 pneumatic fracturing technology, which can further improve the fracture propagation ability of rocks and improve the fracturing effect. From the technical realization point of view, the SC-CO_2 compound fracturing technology is relatively mature and has been applied in practice. At present, the SC-CO_2 jet fracturing technology and the SC-CO_2 pneumatic fracturing technology have been extensively studied in the laboratory, but still need further to be developed from the field application.

In the research of SC-CO_2 fracturing technology, SC-CO_2 energy accumulation fracturing and SC-CO_2 transient high pressure fracturing have also attracted extensive attention recently. SC-CO_2 cumulative fracturing can realize multiple and continuous injection of SC-CO_2 under high pressure. It can overcome the problems of single fracture in hydraulic fracturing technology and small fracture scale caused by high pressure gas blasting, which has been studied in coalbed methane and conglomerate reservoirs. SC-CO_2 transient high pressure fracturing technology has also been explored in coalbed methane. It is worth noting that SC-CO_2 transient high pressure fracturing is similar to pneumatic fracturing: injecting CO_2

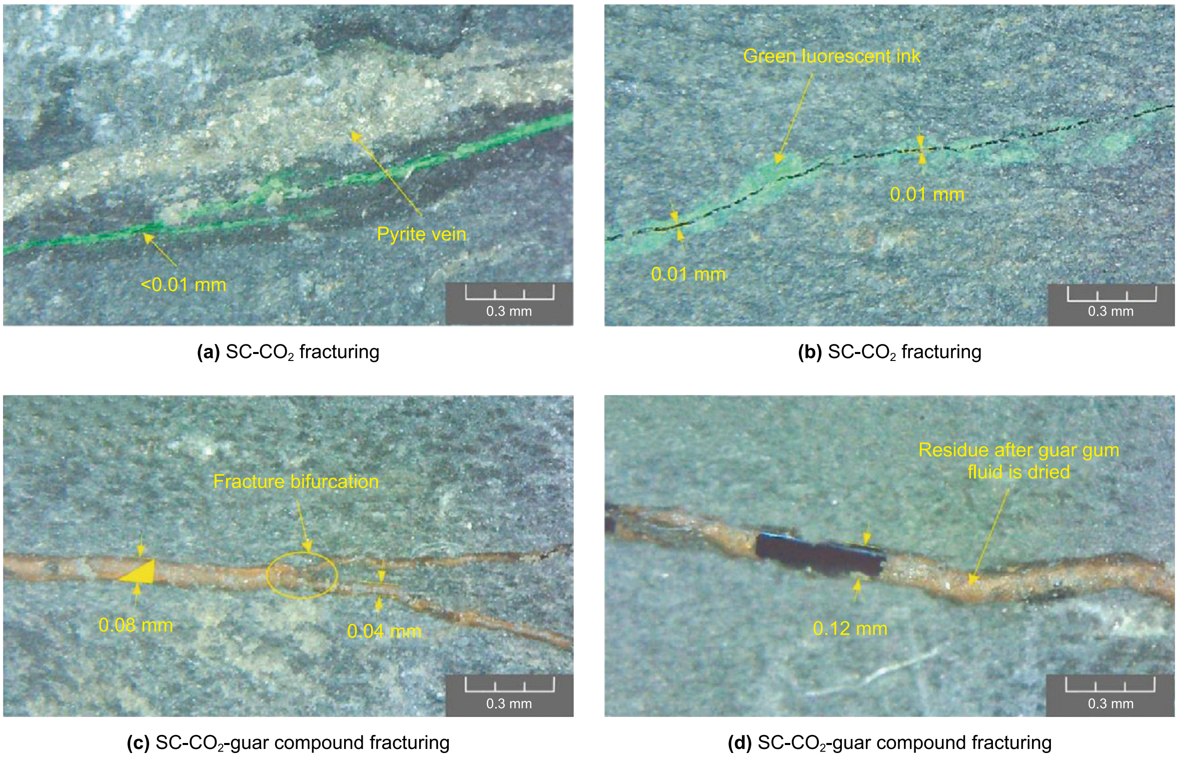

Fig. 17. Fracture width observed by digital microscope (Chen et al., 2021).

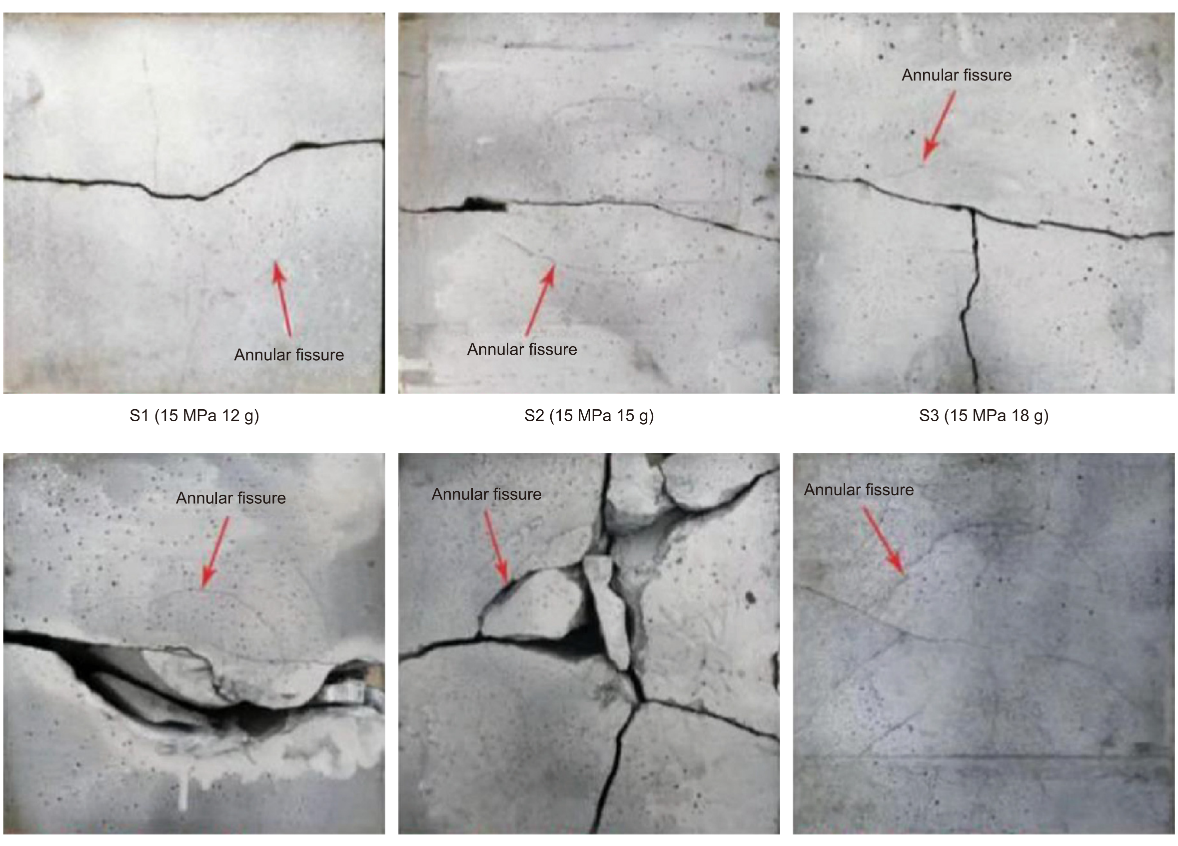

Fig. 18. Schematic diagram of annular fracture (Wang et al., 2023).

into the fracturing pipe, and making the internal pressure rise to the fracture initiation pressure, at this time, CO_2 is in a supercritical state. On the basis of the principle and effect of these two fracturing technologies, combined with the properties of shale reservoirs, the possibility of SC-CO_2 energy accumulation fracturing and SC-CO_2 high-pressure fracturing in shale patterns can be considered.

SC-CO_2 fracturing technology has broad development prospects in the future. However, it still faces challenges in practical application. In terms of filtration, SC-CO_2 has a low surface tension, which makes it easy to filtrate when it passes through porous media, difficult to form a stable flow state. It is necessary to study new fracturing fluid additives or fracturing fluid formulations to improve their stability and diffusion capacity, so as to achieve better fracturing results. In terms of sand carrying capacity, the viscosity of SC-CO_2 is relatively low, which cannot effectively carry a large number of solid particles. It is not easy to form a stable suspension state, which is prone to sedimentation and separation. A new type of environmentally friendly tackifier can be considered to develop currently. In the future, with the development of nanofiber technology, a breakthrough will be made in tackifying ultra-short fibers, realizing stable sand carrying of fracturing fluid and effective support for fractures. In terms of friction resistance, the flow friction of SC-CO_2 in the wellbore is significantly higher than that of conventional water-based fracturing fluid. Especially in the nozzle injection stage, the friction resistance of SC-CO_2 fracturing is greater, which requires a larger construction pressure to meet the displacement requirements, resulting in frequent overpressure of ground equipment and affecting normal construction. Therefore, combined with the research and development of tackifiers, drag reducers suitable for SC-CO_2 can be developed. Besides, CO_2 can only reach supercritical state under high temperature and high pressure, so effective transportation and storage is a technical problem. How to improve the transportation and storage technology of CO_2 is a key issue that researchers are actively studying and exploring. SC-CO_2 fracturing technology needs a large amount of CO_2 supply. How to actively seek more effective CO_2 capture and application technologies to improve the efficiency of CO_2 resource acquisition and utilization is an important issue in current environmental protection and sustainable development.

In terms of cost, due to the complex preparation and treatment process of SC-CO_2, it is required to be carried out under high pressure and high temperature conditions, and more equipments and labor costs need to be invested. In addition, SC-CO_2 fracturing technology needs a lot of CO_2 and corrosion-resistant materials, which also increases the costs of transportation, storage and materials. Therefore, reducing the cost of fracturing technology and improving its economic benefits are the key to future development. In terms of environment, although SC-CO_2 fracturing technology has advantages in reducing water resources use and greenhouse gas emissions compared with traditional fracturing technology, there are still some potential risks. The leakage and emission of CO_2 may have a negative impact on the environment. Therefore, it is necessary to strengthen the management of SC-CO_2 fracturing technology, and ensure the safe transportation and storage of SC-CO_2 to realize safe and sustainable development to the greatest extent.

The future development trend of SC-CO_2 fracturing includes improving fracturing fluid, optimizing proppant and improving reservoir modeling accuracy, so as to improve oil and gas production efficiency. By studying new gas storage materials, improving the design of transportation pipelines and enhancing the sealing performance of CO_2, the safe transportation and storage of CO_2 can be ensured. These measures will further promote the application and rapid development of SC-CO_2 fracturing technology in the field. At the same time, it is necessary to actively respond to related auxiliary problems, such as the prediction of wellbore pressure and temperature, hydrate prevention and control, etc., to improve the maturity of the technology, and also meet the large-scale development needs of unconventional oil and gas.

6. Conclusion

SC-CO_2 fracturing fluid has unique physical and chemical properties. Compared with other waterless fracturing, SC-CO_2 fracturing technology has better fracturing effect on unconventional reservoirs. In this paper, the positive effects of physical properties of SC-CO_2 on fracture initiation and propagation are reviewed. The main mechanism of SC-CO_2 on fracture initiation and fracture propagation in shale is analyzed. In addition, the effects of shale characteristics, natural fractures, proppant migration, temperature and pressure, CO_2 concentration and injection rate on the initiation and propagation of SC-CO_2 in shale are clarified. The optimization of SC-CO_2 fracturing technology, thickener and proppant are discussed to improve the efficiency of SC-CO_2 fracturing. Some new technologies, such as SC-CO_2 jet fracturing, compound fracturing and pneumatic fracturing, are summarized, which provide a new way to improve the fracture propagation effect in shale. However, due to the different characteristics of underground reservoirs and the special properties of SC-CO_2, various problems and challenges will be faced during fracturing. Therefore, the limitations of technology and cost are listed, and some suggestions and expectations for basic research and fracturing technology are put forward. It is believed that with the continuous development and improvement of technology, SC-CO_2 fracturing technology will play an increasingly important role in the development of unconventional oil and gas reservoirs, and further provide new ideas and technical support for oil and gas exploration and development.

CRediT authorship contribution statement

Yuan-Xiu Sun: Writing – original draft, Methodology, Investigation, Conceptualization. **Xiao-Long Wang:** Writing – review & editing, Validation, Formal analysis, Data curation. **Yan-Zhao Meng:** Methodology, Investigation. **Jin-Long Tian:** Resources, Investigation. **Cheng-Hui Lu:** Funding acquisition, Formal analysis.

Declaration of interest statement

There are no conflicts to declare.

References

Akono, A.T., Druhan, J.L., Dávila, G., et al., 2019. A review of geochemical–mechanical impacts in geological carbon storage reservoirs. Greenhouse Gases: Sci. Technol. 9 (3), 474–504. https://doi.org/10.1002/ghg.1870.

Alemu, B.L., Aagaard, P., Munz, I.A., et al., 2011. Caprock interaction with CO_2: a laboratory study of reactivity of shale with supercritical CO_2 and brine. Appl. Geochem. 26 (12), 1975–1989. https://doi.org/10.1016/j.apgeochem.2011.06.028.

Ao, X., Lu, Y.Y., Tang, J.R., et al., 2017. Investigation on the physics structure and chemical properties of the shale treated by supercritical CO_2. J. CO_2 Util. 20, 274–281. https://doi.org/10.1016/j.jcou.2017.05.028.

Ao, X., Qi, Z.L., Xiang, Z.P., et al., 2020. Swelling of shales by supercritical carbon dioxide and its relationship to sorption. ACS Omega 5 (31), 19606–19614. https://doi.org/10.1021/acsomega.0c02118.

Bahrami, H., Rezaee, R., Clennell, B., 2012. Water blocking damage in hydraulically fractured tight sand gas reservoirs: an example from Perth Basin, Western Australia. J. Petrol. Sci. Eng. 88–89, 100–106. https://doi.org/10.1016/j.petrol.2012.04.002.

Bandara, K.M.A.S., Ranjith, P.G., Rathnaweera, T.D., et al., 2021. Crushing and embedment of proppant packs under cyclic loading: an insight to enhanced unconventional oil/gas recovery. Geosci. Front. 12 (6), 100970. https://doi.org/10.1016/j.gsf.2020.02.017.

Bazin, B., Bekri, S., Vizika, O., et al., 2010. Fracturing in tight gas reservoirs: application of special-core-analysis methods to investigate formation-damage mechanisms. SPE J. 15, 969–976. https://doi.org/10.2118/112460-pa.
Bhandari, A.R., Flemings, P.B., Polito, P.J., et al., 2015. Anisotropy and stress dependence of permeability in the barnett shale. Transport Porous Media 108 (2), 393–411. https://doi.org/10.1007/s11242-015-0482-0.
Bhuiyan, M.H., Agofack, N., Gawel, K.M., et al., 2020. Micro- and macroscale consequences of interactions between CO_2 and shale rocks. Energies 13 (5), 1167. https://doi.org/10.3390/en13051167.
Busch, A., Bertier, P., Gensterblum, Y., et al., 2016. On sorption and swelling of CO_2 in clays. Geomech. Geophy. Geo-Energy. Geo-Res. 2 (2), 111–130. https://doi.org/10.1007/s40948-016-0024-4.
Cai, C., Kang, Y., Wang, X.C., et al., 2018. Mechanism of supercritical carbon dioxide (SC-CO_2) hydro-jet fracturing. J. CO_2 Util. 26, 575–587. https://doi.org/10.1016/j.jcou.2018.06.012.
Cai, C., Kang, Y., Wang, X.C., et al., 2019. Experimental study on shale fracturing enhancement by using multi-times pulse supercritical carbon dioxide (SC-CO_2) jet. J. Petrol. Sci. Eng. 178, 948–963. https://doi.org/10.1016/j.petrol.2019.04.009.
Cai, C., Li, B.R., Zhang, Y.Y., et al., 2022. Fracture propagation and induced strain response during supercritical CO_2 jet fracturing. Petrol. Sci. 19 (4), 1682–1699. https://doi.org/10.1016/j.petsci.2022.03.019.
Cai, C., Wang, X.C., Mao, S., Hua, et al., 2017. Heat transfer characteristics and prediction model of supercritical carbon dioxide (SC-CO_2) in a vertical tube. Energies 10 (11), 1870. https://doi.org/10.3390/en10111870.
Cai, C.Z., Li, G.S., Huang, Z.W., et al., 2014. Experimental study of the effect of liquid nitrogen cooling on rock pore structure. J. Nat. Gas Sci. Eng. 21, 507–517. https://doi.org/10.1016/j.jngse.2014.08.026.
Cai, X., Liu, W., Wang, X.X., 2021. Hydromechanical-Coupled cohesive interface simulation of complex fracture network induced by hydrofracturing with low-viscosity supercritical CO_2. Lithosphere 2021 (Special 1). https://doi.org/10.2113/2021/6689981.
Cao, S.G., Zhang, Z.G., Li, Y., et al., 2013. Experimental study of deformation properties of outburst-prone coal induced by gas adsorption and desorption. Meitan Xuebao/J. China Coal Soc. 38 (10), 1792–1799. https://doi.org/10.13225/j.cnki.jccs.2013.10.023.
Chen, H., Hu, Y., Kang, Y., et al., 2019. Fracture initiation and propagation under different perforation orientation angles in supercritical CO_2 fracturing. J. Petrol. Sci. Eng. 183, 106403. https://doi.org/10.1016/j.petrol.2019.106403.
Chen, H., Hu, Y., Kang, Y., et al., 2021. Advantages of supercritical CO_2 compound fracturing in shale on fracture geometry, complexity and width. J. Nat. Gas Sci. Eng. 93, 104033. https://doi.org/10.1016/j.jngse.2021.104033.
Chen, H., Kang, Y., Jin, W.C., et al., 2024. Numerical modeling of fracture propagation of supercritical CO_2 compound fracturing. J. Rock Mech. Geotech. Eng. 16 (7), 2607–2628. https://doi.org/10.1016/j.jrmge.2023.11.043.
Chen, L.Q., Tian, S.C., Li, G.S., et al., 2015. Initiation pressure models for supercritical CO_2 fracturing and sensitivity analysis. Rock Soil Mech. 36 (S2), 125–131. https://doi.org/10.16285/j.rsm.2015.S2.016.
Chen, Y.Q., Nagaya, Y.Y., Ishida, T., 2015. Observations of fractures induced by hydraulic fracturing in anisotropic granite. Rock Mech. Rock Eng. 48 (4), 1455–1461. https://doi.org/10.1007/s00603-015-0727-9.
Cheng, P., Zhang, C.P., Ma, Z.Y., et al., 2022. Experimental study of micromechanical properties alterations of shale matrix treated by ScCO_2-Water saturation using nanoindentation tests. Energy 242, 122965. https://doi.org/10.1016/j.energy.2021.122965.
Cheng, Y.G., Zeng, M.R., Lu, Z.H., et al., 2020. Effects of supercritical CO_2 treatment temperatures on mineral composition, pore structure and functional groups of shale: implications for CO_2 sequestration. Sustainability 12 (9), 3927. https://doi.org/10.3390/su12093927.
Choi, C.S., Cheon, D.S., Song, J.J., 2017. Effect of pore and confining pressure on the supercritical CO_2 permeability of sandstone: implications for the effective pressure law. J. Geophys. Res. Solid Earth 122 (8), 6231–6246. https://doi.org/10.1002/2017jb014475.
Cipolla, C.L., Warpinski, N.R., Mayerhofer, M.J., et al., 2008. The relationship between fracture complexity, reservoir properties, and fracture treatment design. SPE Annual Technical Conference and Exhibition. https://doi.org/10.2118/115769-pa.
Clarkson, C.R., Bustin, R.M., 2000. Binary gas adsorption/desorption isotherms: effect of moisture and coal composition upon carbon dioxide selectivity over methane. Int. J. Coal Geol. 42 (4), 241–271. https://doi.org/10.1016/s0166-5162(99)00032-4.
Cong, Z.Y., Li, Y.W., Pan, Y.S., et al., 2022. Study on CO_2 foam fracturing model and fracture propagation simulation. Energy 238 (Part B), 121778. https://doi.org/10.1016/j.energy.2021.121778.
Daniel, J.K., 2009. The importance of shale composition and pore structure upon gas storage potential of shale gas reservoirs. Mar. Petrol. Geol. 26 (6), 916–927. https://doi.org/10.1016/j.marpetgeo.2008.06.004.
Danso, D.K., Negash, B.M., Ahmed, T.Y., et al., 2021. Recent advances in multifunctional proppant technology and increased well output with micro and nano proppants. J. Petrol. Sci. Eng. 196, 108026. https://doi.org/10.1016/j.petrol.2020.108026.
Denneyd, 2010. Thirty years of gas-shale fracturing:what have we learned? J. Petrol. Technol. 62 (11), 88–90. https://doi.org/10.2118/1110-0088-jpt.
Desimone, J.M., Guan, Z., Elsbernd, C.S., 1992. Synthesis of fluoropolymers in supercritical carbon dioxide. Science 257 (5072), 945–947. https://doi.org/10.1126/science.257.5072.945.
Doherty, M.D., Lee, J.J., Dhuwe, A., et al., 2016. Small molecule cyclic amide and urea based thickeners for organic and SC-CO_2/organic solutions. Energy & Fuels 30 (7), 5601–5610. https://doi.org/10.1021/acs.energyfuels.6b00859.
Dowding, C.H., Hamdi, E., Aimone-Martin, C.T., 2016. Strains induced in urban structures by ultra-high frequency blasting rock motions: a case study. Rock Mech. Rock Eng. 49 (10), 4073–4090. https://doi.org/10.1007/s00603-016-0921-4.
Du, M.Y., Sun, X., Dai, C.L., et al., 2018. Laboratory experiment on a toluene-polydimethyl silicone thickened supercritical carbon dioxide fracturing fluid. J. Petrol. Sci. Eng. 166, 369–374. https://doi.org/10.1016/j.petrol.2018.03.039.
Du, Y., Pang, F., Chen, K., et al., 2019. Experiment of breaking shale using supercritical carbon dioxide jet. Earth Sci. 44 (11), 3749–3756. https://doi.org/10.3799/dqkx.2019.221.
Erarslan, N., Williams, D.J., 2012. Mixed-mode fracturing of rocks under static and cyclic loading. Rock Mech. Rock Eng. 46 (5), 1035–1052. https://doi.org/10.1007/s00603-012-0303-5.
Espinoza, D.N., Santamarina, J.C., 2010. Water-CO_2-mineral systems: interfacial tension, contact angle, and diffusion—implications to CO_2 geological storage. Water Resour. Res. 46 (7), 58–72. https://doi.org/10.1029/2009wr008634.
Fu, M.L., Huang, Q., Gu, Y.A., et al., 2020. Development of novel silicon-based thickeners for a supercritical CO_2 fracturing fluid and study on its rheological and frictional drag behavior. Energy & Fuels 34 (12), 15752–15762. https://doi.org/10.1021/acs.energyfuels.0c01963.
Gan, Q., Elsworth, D., Alpern, J.S., et al., 2015. Breakdown pressures due to infiltration and exclusion in finite length boreholes. J. Petrol. Sci. Eng. 127, 329–337. https://doi.org/10.1016/j.petrol.2015.01.011.
Gibbs, J.W., 1967. On the equilibrium of heterogeneous substances. Trans Connecticut Acad 16 (95), 818–824. https://doi.org/10.2475/ajs.s3-16.96.441.
Goldstein, B., VanZeeland, A., 2015. Self-suspending proppant transport technology increases stimulated reservoir volume and reduces proppant pack and formation damage. SPE Annual Tech. Conf. Exhibition. https://doi.org/10.2118/174867-ms.
Gunter, W.D., Wiwehar, B., Perkins, E.H., 1997. Aquifer disposal of CO_2-rich greenhouse gases: extension of the time scale of experiment for CO_2-sequestering reactions by geochemical modelling. Mineral. Petrol. 59 (1), 121–140. https://doi.org/10.1007/BF01163065.
Guo, T.K., Zhang, Y.L., Shen, L., et al., 2022. Numerical study on the law of fracture propagation in supercritical carbon dioxide fracturing. J. Petrol. Sci. Eng. 208 (Part A), 109369. https://doi.org/10.1016/j.petrol.2021.109369.
Gutierrez, M., Katsuki, D., Tutuncu, A., 2015. Determination of the continuous stress-dependent permeability, compressibility and poroelasticity of shale. Mar. Petrol. Geol. 68, 614–628. https://doi.org/10.1016/j.marpetgeo.2014.12.002.
Hasanipanah, M., Jahed Armaghani, D., Monjezi, M., et al., 2016. Risk assessment and prediction of rock fragmentation produced by blasting operation: a rock engineering system. Environ. Earth Sci. 75, 808. https://doi.org/10.1007/s12665-016-5503-y.
Hashemi, S.S., Zoback, M.D., 2021. Permeability evolution of fractures in shale in the presence of supercritical CO_2. J. Geophys. Res. Solid Earth 126 (8), e2021JB022266. https://doi.org/10.1029/2021jb022266.
He, J.M., Zhang, Y.X., Li, X., et al., 2019. Experimental investigation on the fractures induced by hydraulic fracturing using freshwater and supercritical CO_2 in shale under uniaxial stress. Rock Mech. Rock Eng. 52 (10), 3585–3596. https://doi.org/10.1007/s00603-019-01820-w.
He, J.M., Zhang, Y.X., Yin, C., et al., 2020. Hydraulic fracturing behavior in shale with water and supercritical CO_2 under triaxial compression. Geofluids 2020, 1–10. https://doi.org/10.1155/2020/4918087.
He, Y.T., Yang, Z.Z., Jiang, Y.F., et al., 2020. A full three-dimensional fracture propagation model for supercritical carbon dioxide fracturing. Energy Sci. Eng. 8 (8), 2894–2906. https://doi.org/10.1002/ese3.709.
He, Z.G., Tian, S.C., Li, G.S., et al., 2015. The pressurization effect of jet fracturing using supercritical carbon dioxide. J. Nat. Gas Sci. Eng. 27, 842–851. https://doi.org/10.1016/j.jngse.2015.09.045.
Heller, R., Vermylen, J., Zoback, M., 2014. Experimental investigation of matrix permeability of gas shales. AAPG (Am. Assoc. Pet. Geol.) Bull. 98 (5), 975–995. https://doi.org/10.1306/09231313023.
Hou, B., Yeerfulati, M., Fu, W.N., et al., 2020. Experimental study on the hydraulic fracture propagation for shale temporary plugging and diverting fracturing. J. Liaon. Shihua Univ. 40 (4), 98–104. https://doi.org/10.3969/j.issn.1672-6952.2020.04.014 (in Chinese).
Hou, L., Elsworth, D., Wang, J., et al., 2024. Feasibility and prospects of symbiotic storage of CO_2 and H_2 in shale reservoirs. Renew. Sustain. Energy Rev. 189, 113878. https://doi.org/10.1016/j.rser.2023.113878.
Hou, X.Q., Lu, Y.J., Fang, B., et al., 2023. Research progress on application of surfactants in unconventional oil and gas stimulation. Petrochem. Technol. 52 (5), 734–741. https://doi.org/10.3969/j.issn.1000-8144.2023.05.020.
Hou, Z.K., Yang, C.H., Guo, Y.T., et al., 2015. Experimental Study on Anisotropic Properties of Longmaxi Formation Shale under Uniaxial Compression. Rock and Soil Mechanics 36 (9), 2541–2550. https://doi.org/10.16285/j.rsm.2015.09.014.
Hou, Z.K., Yuan, Y., Chen, Y., et al., 2024. A review of supercritical CO_2 fracturing technology in shale gas reservoirs. Processes 12 (6), 1238. https://doi.org/10.3390/pr12061238.
Hu, S.B., Pang, S.G., Yan, Z.Y., 2019. A new dynamic fracturing method: deflagration fracturing technology with carbon dioxide. Int. J. Fract. 220 (1), 99–111. https://doi.org/10.1007/s10704-019-00403-8.
Hu, Y., Kang, Y., Wang, X.C., et al., 2016. Experimental and theoretical analysis of a

supercritical carbon dioxide jet on wellbore temperature and pressure. J. Nat. Gas Sci. Eng. 36, 108–116. https://doi.org/10.1016/j.jngse.2016.10.014.

Hu, Y., Liu, Y.W., Cai, C., et al., 2017. Fracture initiation of an inhomogeneous shale rock under a pressurized supercritical CO_2 jet. Appl. Sci. 7 (10), 1093. https://doi.org/10.3390/app7101093.

Huang, Z.W., Zhang, S.K., Yang, R.Y., et al., 2020. A review of liquid nitrogen fracturing technology. Fuel 266, 117040. https://doi.org/10.1016/j.fuel.2020.117040.

Hui, D., Pan, Y., Luo, P.Y., et al., 2019. Effect of supercritical CO_2 exposure on the high-pressure CO_2 adsorption performance of shales. Fuel 247, 57–66. https://doi.org/10.1016/j.fuel.2019.03.013.

Inui, S., Ishida, T., Chen, Q., et al.. AE monitoring of hydraulic fracturing experiment in granite blocks using supercritical CO_2. Water and Viscous Oil. https://api.semanticscholar.org/Corpusid:132296799.

Isaka, B.L.A., Ranjith, P.G., Rathnaweera, T.D., et al., 2019. Testing the frackability of granite using supercritical carbon dioxide: insights into geothermal energy systems. J. CO_2 Util. 34, 180–197. https://doi.org/10.1016/j.jcou.2019.06.009.

Ishida, T., Aoyagi, K., Niwa, T., et al., 2012. Acoustic emission monitoring of hydraulic fracturing laboratory experiment with supercritical and liquid CO_2. Geophys. Res. Lett. 39 (16). https://doi.org/10.1029/2012gl052788.

Ishida, T., Chen, Y.Q., Bennour, Z., et al., 2016. Features of CO_2 fracturing deduced from acoustic emission and microscopy in laboratory experiments. J. Geophys. Res. Solid Earth 121 (11), 8080–8098. https://doi.org/10.1002/2016jb013365.

Ito, T., 2008. Effect of pore pressure gradient on fracture initiation in fluid saturated porous media: rock. Eng. Fract. Mech. 75 (7), 1753–1762. https://doi.org/10.1016/j.engfracmech.2007.03.028.

Jia, Y.Z., Lu, Y.Y., Elsworth, D., et al., 2018. Surface characteristics and permeability enhancement of shale fractures due to water and supercritical carbon dioxide fracturing. J. Petrol. Sci. Eng. 165, 284–297. https://doi.org/10.1016/j.petrol.2018.02.018.

Jiang, Y., Luo, Y., Lu, Y., et al., 2016. Effects of supercritical CO_2 treatment time, pressure, and temperature on microstructure of shale. Energy 97, 173–181. https://doi.org/10.1016/j.energy.2015.12.124.

Jiang, Y.D., Qin, C., Kang, Z.P., et al., 2018. Experimental study of supercritical CO_2 fracturing on initiation pressure and fracture propagation in shale under different triaxial stress conditions. J. Nat. Gas Sci. Eng. 55, 382–394. https://doi.org/10.1016/j.jngse.2018.04.022.

Kang, Y.Z., 2012. Characteristics and exploration prospect of unconventional shale oil and gas reservoirs in China. Nat. Gas. Ind. 32 (4), 1–5+117. https://doi.org/10.3787/j.issn.1000-0976.2012.04.001.

Kang, Y.Z., Zhou, L., 2016. Strategic thinking on unconventional oil and gas in China. Earth Sci. Front. 23 (2), 1–7. https://doi.org/10.13745/j.esf.2016.02.001.

Kargbo, D.M., Wilhelm, R.G., Campbell, D.J., 2010. Natural gas plays in the Marcellus shale: challenges and potential opportunities. Environ. Sci. Technol. 44, 5679–5684. https://doi.org/10.1021/es903811p.

Khosrokhavar, R., Wolf, K.H., Bruining, H., 2014. Sorption of CH_4 and CO_2 on a carboniferous shale from Belgium using a manometric setup. Int. J. Coal Geol. 128, 153–161. https://doi.org/10.1016/j.coal.2014.04.014.

King, 2010. Thirty Years of Gas Shale Fracturing: what Have We Learned? Society of Petroleum Engineers. https://doi.org/10.2118/133456-ms.

Kizaki, A., Tanaka, H., Sakaguchi, K., 2013. Hydraulic fracturing in inada granite and ogino tuff using super critical carbon dioxide and water as fracturing fluids. J. MMIJ 129 (7), 461–466 https://doi.org/10.2473./journalofmmij.129.461.

Kohli, A.H., Zoback, M.D., 2013. Frictional properties of shale reservoir rocks. J. Geophys. Res. Solid Earth 118 (9), 5109–5125. https://doi.org/10.1002/jgrb.50346.

Kolle, J.J., Marvin, M.H., 2000. Jet-assisted drilling with supercritical carbon dioxide. SPE J. US6347675 B1.

Kumar, D., Gonzalez, R.A., Ghassemi, A., 2019. The role of micro-proppants in conductive fracture network development. Society of Petroleum Engineers. SPE Hydraulic Fracturing Technology Conference and Exhibition. https://doi.org/10.2118/194340-ms.

Li, B., Mou, J., Zhang, S., et al., 2022. Experimental study on the interaction between CO_2 and rock during CO_2 pre-pad energized fracturing operation in thin interbedded shale. Front. Energy Res. 10–2022. https://doi.org/10.3389/fenrg.2022.825464.

Li, B.F., Zheng, C., Ding, L.P., et al., 2018. Design and application of measuring system for CO_2 filtration performance under high pressure. Res. Explor. Lab. 37 (2), 76–79 cnki:sun:sysy.0.2018-02-019 (in Chinese).

Li, G., Wang, H., Shen, Z., et al., 2013. Application investigations and prospects of supercritical carbon dioxide jet in petroleum engineering. J. China Univ. Petroleum 37 (5), 76–80+87. https://doi.org/10.3969/j.issn.1673-5005.2013.05.011 (in Chinese).

Li, G.S., Wang, H.Z., Shen, Z.H., et al., 2013. Application investigations and prospects of supercritical carbon dioxide jet in petroleum engineering. J. China Univ. Petroleum 37 (5), 76–80+87. https://doi.org/10.3969/j.issn.1673-5005.2013.05.011 (in Chinese).

Li, Q.C., Liu, J., Wang, S.M., et al., 2024. Numerical insights into factors affecting collapse behavior of horizontal wellbore in clayey silt hydrate-bearing sediments and the accompanying control strategy. Ocean. Eng. 297, 117029. https://doi.org/10.1016/j.oceaneng.2024.117029.

Li, S.H., Zhang, S.C., Ma, X.F., et al., 2019a. Hydraulic fractures induced by water-/carbon dioxide-based fluids in tight sandstones. Rock Mech. Rock Eng. 52 (9), 3323–3340. https://doi.org/10.1007/s00603-019-01777-w.

Li, S.H., Zhang, S.C., Ma, X.F., et al., 2019b. Coupled physical–chemical effects of CO_2 on rock properties and breakdown during intermittent CO_2-hybrid fracturing. Rock Mech. Rock Eng. 53 (4), 1665–1683. https://doi.org/10.1007/s00603-019-02000-6.

Li, S.H., Zhang, S.C., Zou, Y.S., et al., 2020. Experimental study on the feasibility of supercritical CO_2-gel fracturing for stimulating shale oil reservoirs. Eng. Fract. Mech. 238. https://doi.org/10.1016/j.engfracmech.2020.107276.

Li, X.J., Li, G.S., Yu, W., et al., 2018. Thermal effects of liquid/supercritical carbon dioxide arising from fluid expansion in fracturing. SPE J. 23 (6), 2026–2040. https://doi.org/10.2118/191357-pa.

Li, Y.W., Zhang, J., Liu, Y., 2015. Effects of loading direction on failure load test results for Brazilian tests on coal rock. Rock Mech. Rock Eng. 49 (6), 2173–2180. https://doi.org/10.1007/s00603-015-0841-8.

Liang, F., Sayed, M., Al-Muntasheri, G.A., et al., 2016. A comprehensive review on proppant technologies. Petroleum 2 (1), 26–39. https://doi.org/10.1016/j.petlm.2015.11.001.

Liang, G.W., He, W., Yan, J.W., 2022. Weakening and fracturing mechanism of mechanical properties of coal and rock caused bysupercritical CO_2. J. China Coal Soc. 47 (7), 2557–2568. https://doi.org/10.13225/j.cnki.jccs.yg21.1899.

Liao, Y., 2021. Experimental research review of supercritical carbon dioxide fracturing technology. China Mine Eng. 50 (2), 45–47. https://doi.org/10.19607/j.cnki.cn11-5068/tf.2021.02.013.

Liu, B.L., Suzuki, A., Ito, T., 2020. Numerical analysis of different fracturing mechanisms between supercritical CO_2 and water-based fracturing fluids. Int. J. Rock Mech. Min. Sci. 132. https://doi.org/10.1016/j.ijrmms.2020.104385.

Liu, G.J., Shang, D.L., Chu, P., et al., 2024. Thermomechanical coupling seepage in fractured shale under stimulation of supercritical carbon dioxide. Front. Earth Sci. 12. https://doi.org/10.3389/feart.2024.1399806.

Liu, G.J., Xian, X.F., Zhou, J.P., 2017. Experimental study on the supercritical CO_2 fracturing of shale. J. China Coal Soc. 42 (3), 694–701. https://doi.org/10.13225/j.cnki.jccs.2016.06040 (in Chinese).

Liu, H.L., Li, C.X., Sun, J.F., et al., 2018. The productivity analysis of vertical well with partial penetration fracture in tight sandstone reservoir. J. Liaon. Shihua Univ. 38 (1), 37–44+59. https://doi.org/10.3969/j.issn.1672-6952.1018.01.007 (in Chinese).

Liu, L.Y., Zhu, W.C., Wei, C.H., et al., 2018. Microcrack-based geomechanical modeling of rock-gas interaction during supercritical CO_2 fracturing. J. Petrol. Sci. Eng. 164, 91–102. https://doi.org/10.1016/j.petrol.2018.01.049.

Liu, S.C., Zhao, M.W., Wu, Y.N., et al., 2022. Development and performance evaluation of a novel silica nanoparticle-reinforced CO_2-sensitive fracturing fluid with high temperature and shear resistance ability. Energy & Fuels 36 (13), 7177–7185. https://doi.org/10.1021/acs.energyfuels.2c01056.

Liu, W.B., Xu, X.Y., Liu, C., et al., 2022. The stimulation mechanism and performance analysis of supercritical CO_2 and hydraulic sand-carrying composite volume fracturing technology on continental shale reservoirs. Acta Pet. Sin. 43 (3), 399–409. https://doi.org/10.7623/syxb202203007 (in Chinese).

Louk, K., Ripepi, N., Luxbacher, K., et al., 2017. Monitoring CO_2 storage and enhanced gas recovery in unconventional shale reservoirs: results from the Morgan County, Tennessee injection test. J. Nat. Gas Sci. Eng. 45, 11–25. https://doi.org/10.1016/j.jngse.2017.03.025.

Lu, J., Nicot, J.-P., Mickler, P.J., et al., 2016. Alteration of Bakken reservoir rock during CO_2-based fracturing—an autoclave reaction experiment. J. Unconvent. Oil. Gas Res. 14, 72–85. https://doi.org/10.1016/j.juogr.2016.03.002.

Lu, Y., Zhou, J., Xian, X., et al., 2021. Research progress and prospect of the integrated supercritical CO_2 enhanced shale gas recovery and geological sequestration. Nat. Gas. Ind. 41 (6), 60–73. https://doi.org/10.3787/j.issn.1000-0976.2021.06.007 (in Chinese).

Lu, Y.Y., Ao, X., Tang, J.R., et al., 2016. Swelling of shale in supercritical carbon dioxide. J. Nat. Gas Sci. Eng. 30, 268–275. https://doi.org/10.1016/j.jngse.2016.02.011.

Lu, Y.Y., Chen, X.Y., Tang, J.R., et al., 2019. Relationship between pore structure and mechanical properties of shale on supercritical carbon dioxide saturation. Energy 172, 270–285. https://doi.org/10.1016/j.energy.2019.01.063.

Lu, Y.Y., Liao, Y., Tang, J.R., et al., 2018. Experimental study on fracture initiation pressure and morphology in shale using supercritical CO_2 fracturing. J. China Coal Soc. 43 (1), 175–180. https://doi.org/10.13225/j.cnki.jccs.2017.0580 (in Chinese).

Luo, T.T., Wang, J.G., Chen, L., et al., 2024. Quantitative characterization of the brittleness of deep shales by integrating mineral content, elastic parameters, in situ stress conditions and logging analysis. Int. J. Coal Sci. Tech. 11 (10). https://doi.org/10.1007/s40789-023-00637-x.

Luo, Z.F., Zhang, N.L., Zhao, L.Q., et al., 2020. Chemical proppant generated in the fracture from the novel fracturing fluid system. SPE Canada Unconventional Resources Conference. https://doi.org/10.2118/200004-ms.

Lyu, Q., Long, X.P., Ranjith, P.G., et al., 2018. Experimental investigation on the mechanical properties of a low-clay shale with different adsorption times in sub-/super-critical CO_2. Energy 147, 1288–1298. https://doi.org/10.1016/j.energy.2018.01.084.

Lyu, Q., Ranjith, P.G., Long, X., et al., 2016. Experimental investigation of mechanical properties of black shales after CO_2-water-rock interaction. Materials 9 (8), 663. https://doi.org/10.3390/ma9080663.

Lyu, Q., Ranjith, P.G., Long, X.P., et al., 2015. A review of shale swelling by water adsorption. J. Nat. Gas Sci. Eng. 27, 1421–1431. https://doi.org/10.1016/j.jngse.2015.10.004.

Ma, X.P., Mu, H.L., Guo, S.G., 2021. Synthesis and performance evaluation of viscoelastic surfactant for fracturing fluid. Chin. J. Appl. Chem. 38 (8), 923–932. https://doi.org/10.19894/j.issn.1000-0518.200259 (in Chinese).

Marbler, H., Erickson, K.P., Schmidt, M., et al., 2012. Geomechanical and geochemical effects on sandstones caused by the reaction with supercritical CO_2: an experimental approach to in situ conditions in deep geological reservoirs. Environ. Earth Sci. 69 (6), 1981–1998. https://doi.org/10.1007/s12665-012-2033-0.
Memon, S., Feng, R.H., Ali, M., et al., 2022. Supercritical CO_2-Shale interaction induced natural fracture closure: implications for scCO_2 hydraulic fracturing in shales. Fuel 313, 122682. https://doi.org/10.1016/j.fuel.2021.122682.
Memon, S., Verrall, M., Lebedev, M., et al., 2024. Nanoscale analysis of shale matrix alteration after supercritical CO_2 treatment: implications for scCO_2 fracturing in shales. Energy & Fuels 38 (3), 1873–1890. https://doi.org/10.1021/acs.energyfuels.3c03291.
Meng, M., Baldino, S., Miska, S.Z., et al., 2019. Wellbore stability in naturally fractured formations featuring dual-porosity/single-permeability and finite radial fluid discharge. J. Petrol. Sci. Eng. 174, 790–803. https://doi.org/10.1016/j.petrol.2018.11.088.
Nguyen, P.D., Dewprashad, B.T., Weaver, J.D., 1998. A new approach for enhancing fracture conductivity. SPE Asia Pacific Oil and Gas Conference and Exhibition. https://doi.org/10.2118/50002-ms.
Ozdemir, E., Schroeder, K., 2009. Effect of moisture on adsorption isotherms and adsorption capacities of CO_2 on coals. Energy & Fuels 23 (28), 21e31. https://doi.org/10.1021/ef801126a.
Pan, Y., Hui, D., Luo, P.Y., et al., 2018a. Experimental investigation of the geochemical interactions between supercritical CO_2 and shale: implications for CO_2 storage in gas-bearing shale formations. Energy & Fuels 32 (2), 1963–1978. https://doi.org/10.1021/acs.energyfuels.7b03074.
Pan, Y., Hui, D., Luo, P.Y., et al., 2018b. Influences of subcritical and supercritical CO_2 treatment on the pore structure characteristics of marine and terrestrial shales. J. CO_2 Util. 28, 152–167. https://doi.org/10.1016/j.jcou.2018.09.016.
Pangilinan, K.D., De Leon, A.C.C., Advincula, R.C., 2016. Polymers for proppants used in hydraulic fracturing. J. Petrol. Sci. Eng. 145, 154–160. https://doi.org/10.1016/j.petrol.2016.03.022.
Patel, S.M., Sondergeld, C.H., Rai, C.S., 2017. Laboratory studies of hydraulic fracturing by cyclic injection. Int. J. Rock Mech. Min. Sci. 95, 8–15. https://doi.org/10.1016/j.ijrmms.2017.03.008.
Peng, P.H., Ju, Y., Wang, Y.L., et al., 2017. Numerical analysis of the effect of natural microcracks on the supercritical CO_2 fracturing crack network of shale rock based on bonded particle models. Int. J. Numer. Anal. Methods GeoMech. 41 (18), 1992–2013. https://doi.org/10.1002/nag.2712.
Qian, Q., Lu, M.J., Zhong, A.H., 2023. Study on fracture morphology of CO_2 energized fracturing of continental shale oil in Dongying Sag. Petrol. Drill. Tech. 51 (5), 42–48. https://doi.org/10.11911/syztjs.2023082.
Qin, C., Jiang, Y., Luo, Y., et al., 2017. Effect of supercritical carbon dioxide treatment time, pressure, and temperature on shale water wettability. Energy & Fuels 31 (1), 493–503. https://doi.org/10.1021/acs.energyfuels.6b03257.
Qin, W.L., Yue, L., Liang, G.Q., et al., 2017. Effect of multi-walled carbon nanotubes on linear viscoelastic behavior and microstructure of zwitterionic wormlike micelle at high temperature. Chem. Eng. Res. Des. 123, 14–22. https://doi.org/10.1016/j.cherd.2017.04.027.
Qin, X.Y., Wang, Z.L., Yu, H.Y., et al., 2016. A new shale brittleness evaluation method based on rock physics and mineral compositions. Nat. Gas Geosci. 27 (10), 1924–1932+1941. https://doi.org/10.11764/j.issn.1672-1926.2016.10.1924 (in Chinese).
Rathnaweera, T.D., Ranjith, P.G., Perera, M.S.A., et al., 2015. CO_2-induced mechanical behaviour of Hawkesbury sandstone in the Gosford basin: an experimental study. Mat. Sci. Eng. A. 641, 123–137. https://doi.org/10.1016/j.msea.2015.05.029.
Rempel, K.U., Liebscher, A., Heinrich, W., et al., 2011. An experimental investigation of trace element dissolution in carbon dioxide: applications to the geological storage of CO_2. Chem. Geol. 289 (3–4), 224–234. https://doi.org/10.1016/j.chemgeo.2011.08.003.
Saldungaray, P., Palisch, T., 2013. Understanding ceramic proppants: are they all created equal? SPE Unconvent. Gas Conf. Exh. https://doi.org/10.2118/164042-ms.
Scanlon, B.R., Reedy, R.C., Nicot, J.P., 2014. Comparison of water use for hydraulic fracturing for unconventional oil and gas versus conventional oil. Environ. Sci. Technol. 48 (20), 12386–12393. https://doi.org/10.1021/es502506v.
Sevinç, A.H., Durgun, M.Y., Eken, M., 2017. A Taguchi approach for investigating the engineering properties of concretes incorporating barite, colemanite, basaltic pumice and ground blast furnace slag. Construct. Build. Mater. 135, 343–351. https://doi.org/10.1016/j.conbuildmat.2016.12.209.
Shen, Z.Q., Wang, Y.L., Jia, W.F., et al., 2022. Static suspended sand performance and mechanism analysis of new CO thickener for low permeability reservoir. Appl. Chem. Ind. 51 (1), 68–72. https://doi.org/10.16581/j.cnki.issn1671-3206.2022.01.012 (in Chinese).
Shi, X., Jiang, S., Wang, Z.X., et al., 2020. Application of nanoindentation technology for characterizing the mechanical properties of shale before and after supercritical CO_2 fluid treatment. J. CO_2 Util. 37, 158–172. https://doi.org/10.1016/j.jcou.2019.11.022.
Song, W.Q., Ni, H.J., Tang, P., et al., 2021. Simulation of supercritical carbon dioxide fracturing in shale gas reservoir. J. Therm. Sci. 30 (4), 1444–1451. https://doi.org/10.1007/s11630-021-1477-5.
Song, X.Z., Li, G.S., Guo, B., et al., 2018. Transport feasibility of proppant by supercritical carbon dioxide fracturing in reservoir fractures. J. Hydrodyn. 30 (3), 507–513. https://doi.org/10.1007/s42241-018-0055-0.
Sparks, D.L., Hernandez, R., Estévez, L.A., 2008. Evaluation of density-based models for the solubility of solids in supercritical carbon dioxide and formulation of a new model. Chem. Eng. Sci. 63 (17), 4292–4301. https://doi.org/10.1016/j.ces.2008.05.031.
Su, J.Z., Li, F.X., Zhou, T., 2019. Hydraulic fracture propagation behavious and geometry under supercritical CO_2 fracturing in shale reservoirs. Oil Gas Geol. 40 (3), 616–625. https://doi.org/10.11743/ogg20190316.
Sun, B.J., Wang, J.T., Sun, W.C., et al., 2019. Advances in fundamental research of supercritical CO_2 fracturing tech nology for unconventional natural gas reservoirs. J. China Univ. Petrol. (Edition of Natural Science) 43 (5), 82–91. https://doi.org/10.3969/j.issn.1673-5005.2019.05.009 (in Chinese).
Sun, Y., He, L., Dong, B., et al., 2024a. The mechanism of proppant transport dynamic propagation in rough fracture for supercritical CO_2 fracturing. Phys. Fluids 36 (10). https://doi.org/10.1063/5.0235273.
Sun, Y., Ma, Y., Yu, B., et al., 2024b. Perspectives on molecular simulation of CO_2/CH_4 competitive adsorption in a shale matrix: a review. Energy & Fuels 38 (17), 15935–15971. https://doi.org/10.1021/acs.energyfuels.4c02206.
Suo, Y., Zhang, X., Tian, Y.J., et al., 2024. Effect of natural fractures with different sizes on the development of supercritical CO_2 fractures – a case study on Songliao Basin. J. CO_2 Util. 82. https://doi.org/10.1016/j.jcou.2024.102761.
Surjaatmadja, J.B., Grundmann, S.R., McDaniel, B., et al., 1998. Hydrajet fracturing: an effective method for placing many fractures in openhole horizontal wells. https://doi.org/10.2118/48856-ms.
Tao, J., Meng, S., Li, D., et al., 2024. Research on evolutionary laws of mechanical properties and pore structure during CO_2 pre-injection fracturing in shale reservoirs. Energies 17 (11), 2470. https://doi.org/10.3390/en17112470.
Tian, S.C., Zhang, P.P., Sheng, M., et al., 2020. Modification of microscopic properties of shale by carbonic acid treatment: implications for CO_2-based fracturing in shale formations. Energy & Fuels 34 (3), 3458–3466. https://doi.org/10.1021/acs.energyfuels.9b03772.
Tian, S.F., Zhou, J.P., Xian, X.F., et al., 2023. Effect of supercritical CO_2 on alteration of tensile strength of shale. J. China Coal Soc. 48 (7), 2728–2736. https://doi.org/10.13225/j.cnki.jccs.cn23.0282 (in Chinese).
Vo, L.K., Nguyen, P.D., Liang, F., et al., 2014. Enhancing proppant pack conductivity with consolidation and agglomeration performance: a laboratory study. SPE International Symposium and Exhibition on Formation Damage Control. https://doi.org/10.2118/168188-ms.
Wang, H.T., Zuo, L., Guo, Y.T., et al., 2021. Effect of carbon dioxide on the degradation of shale mechanical properties. Science Technology and Engineering 21 (29), 12536–12542 (in Chinese).
Wang, H.Z., Li, G., Shen, Z., 2012. A feasibility analysis on shale gas exploitation with supercritical carbon dioxide. Energy Sources, Part A Recovery, Util. Environ. Eff. 34 (15), 1426–1435. https://doi.org/10.1080/15567036.2010.529570.
Wang, H.Z., Li, G.S., Zhu, B., et al., 2019. Key problems and solutions in supercritical CO_2 fracturing technology. Front. Energy 13 (4), 667–672. https://doi.org/10.1007/s11708-019-0626-y.
Wang, H.Z., Wang, M., Yang, B., et al., 2018. Numerical study of supercritical CO_2 and proppant transport in different geometrical fractures. Greenhouse Gases: Sci. Technol. 8 (5), 898–910. https://doi.org/10.1002/ghg.1803.
Wang, J.H., Elsworth, D., Wu, Y., et al., 2017. The influence of fracturing fluids on fracturing processes: a comparison between water, oil and SC-CO_2. Rock Mech. Rock Eng. 51 (1), 299–313. https://doi.org/10.1007/s00603-017-1326-8.
Wang, J.T., Sun, B.J., Li, H., et al., 2018. Phase state control model of supercritical CO_2 fracturing by temperature control. Int. J. Heat Mass Tran. 118, 1012–1021. https://doi.org/10.1016/j.ijheatmasstransfer.2017.11.070.
Wang, J.T., Wang, Z.Y., Sun, B.J., et al., 2019. Optimization design of hydraulic parameters for supercritical CO_2 fracturing in unconventional gas reservoir. Fuel 235, 795–809. https://doi.org/10.1016/j.fuel.2018.08.078.
Wang, K.R., Xu, T.R., Wang, F.G., et al., 2016. Experimental study of CO_2–brine–rock interaction during CO_2 sequestration in deep coal seams. Int. J. Coal Geol. 154–155, 265–274. https://doi.org/10.1016/j.coal.2016.01.010.
Wang, L., Dong, Z., Li, X., et al., 2018. A multi-scale flow model for production performance analysis in shale gas reservoirs with fractal geometry. Sci. Rep. 8 (1), 11464. https://doi.org/10.1038/s41598-018-29710-1.
Wang, L., Yao, B.W., Xie, H.J., et al., 2017. CO_2 injection-induced fracturing in naturally fractured shale rocks. Energy 139, 1094–1110. https://doi.org/10.1016/j.energy.2017.08.031.
Wang, M., Feng, Y.T., Pande, G.N., et al., 2018. A coupled 3-dimensional bonded discrete element and lattice Boltzmann method for fluid-solid coupling in cohesive geomaterials. Int. J. Numer. Anal. Methods GeoMech. 42 (12), 1405–1424. https://doi.org/10.1002/nag.2799.
Wang, S., Javadpour, F., Feng, Q.H., 2016. Confinement correction to mercury intrusion capillary pressure of shale nanopores. Sci. Rep. 6 (1), 20160. https://doi.org/10.1038/srep20160.
Wang, S., Liu, K.Q., Han, J., et al., 2019. Investigation of properties alternation during super-critical CO_2 injection in shale. Appl. Sci. 9 (8). https://doi.org/10.3390/app9081686.
Wang, T., Wang, H., Zhang, F., et al., 2013. Simulation of CO_2–water–rock interactions on geologic CO_2 sequestration under geological conditions of China. Mar. Pollut. Bull. 76 (1), 307–314. https://doi.org/10.1016/j.marpolbul.2013.08.014.
Wang, X., Sun, X., Guo, X., et al., 2024. Study on the influence of supercritical CO_2 with high temperature and pressure on pore-throat structure and minerals of shale. ACS Omega 9 (13), 15259–15270. https://doi.org/10.1021/acsomega.3c09698.
Wang, X.F., Hu, S.B., Wang, E.Y., 2023. Experimental research and fractal analysis of

supercritical CO_2 pneumatic fracturing under true triaxial stress. Energy & Fuels 37 (16), 12113–12122. https://doi.org/10.1021/acs.energyfuels.3c01583.
Wang, X.Z., Wu, J.Q., Zhang, J.T., 2014. Application of CO_2 fracturing technology for terrestrial shale gas reservoirs. Nat. Gas. Ind. 34 (1), 64–67. https://doi.org/10.3787/j.issn.1000-0976.2014.01.009 (in Chinese).
Wang, Y.L., Liu, B., Li, D., et al., 2022. SiO_2 synergistic modification of siloxane thickener to improve the viscosity of supercritical CO_2 fracturing fluid. Energy Sources, Part A Recovery, Util. Environ. Eff. 44 (3), 6602–6617. https://doi.org/10.1080/15567036.2022.2100946.
Wu, W., Zoback, M.D., Kohli, A.H., 2017. The impacts of effective stress and CO_2 sorption on the matrix permeability of shale reservoir rocks. Fuel 203, 179–186. https://doi.org/10.1016/j.fuel.2017.04.103.
Xian, X.F., Yin, H., Zhou, J.P., 2015. A New Experimental Apparatus for Fracturing Shale Gas Reservoir to Enhance Permeability with Supercritical Carbon Dioxide. Journal of Southwest Petroleum University: Science & Technology Edition 37 (3), 1–8. https://doi.org/10.11885/j.issn.1674-5086.2015.02.08.01 (in Chinese).
Xu, S.T., 2023. Study on the Effect of N_2/SC-CO_2 Mixed Gas on the Mechanical Properties of Shale. Liaoning Technical University. https://doi.org/10.27210/d.cnki.glnju.2023.000691 (in Chinese).
Yan, C.L., Deng, J.G., Hu, L.B., et al., 2014. Brittle failure of shale under uniaxial compression. Arabian J. Geosci. 8 (5), 2467–2475. https://doi.org/10.1007/s12517-014-1373-3.
Yan, H., Zhang, J.X., Zhou, N., et al., 2021. Quantitative characterization of crack propagation behavior under the action of stage-by-stage fracturing induced by SC-CO_2 fluid. Eng. Fract. Mech. 256. https://doi.org/10.1016/j.engfracmech.2021.107984.
Yang, J.H., Lu, W.B., Jiang, Q.H., et al., 2016. Frequency comparison of blast-induced vibration per delay for the full-face millisecond delay blasting in underground opening excavation. Tunn. Undergr. Space Technol. 51, 189–201. https://doi.org/10.1016/j.tust.2015.10.036.
Yasuhara, H., Kinoshita, N., Ohfuji, H., et al., 2011. Temporal alteration of fracture permeability in granite under hydrothermal conditions and its interpretation by coupled chemo-mechanical model. Appl. Geochem. 26 (12), 2074–2088. https://doi.org/10.1016/j.apgeochem.2011.07.005.
Ye, L., Zou, Y.S., Zhao, Q.Y., et al., 2018. Experimental research on the CO_2 fracturingfracture propagation laws of high sandstone. Oil Drilling Prod. Technol. 40 (3), 93–100. https://doi.org/10.13639/j.odpt.2018.03.015.
Yin, B., Lou, Y.S., Liu, S.Y., 2024. Mechanism of fracture propagation for SC-CO_2 fracturing and phase-change process. J. CO_2 Util. 80, 102691. https://doi.org/10.1016/j.jcou.2024.102691.
Yin, H., Zhou, J., Jiang, Y., et al., 2016. Physical and structural changes in shale associated with supercritical CO_2 exposure. Fuel 184, 289–303. https://doi.org/10.1016/j.fuel.2016.07.028.
Yin, H., Zhou, J.P., Xian, X.F., et al., 2017. Experimental study of the effects of sub- and super-critical CO_2 saturation on the mechanical characteristics of organic-rich shales. Energy 132, 84–95. https://doi.org/10.1016/j.energy.2017.05.064.
Yu, Z., Liu, L., Yang, S., et al., 2012. An experimental study of CO_2–brine–rock interaction at in situ pressure–temperature reservoir conditions. Chem. Geol. 326–327, 88–101. https://doi.org/10.1016/j.chemgeo.2012.07.030.
Zang, Y.X., Wang, H.Z., Wang, B., et al., 2024. In-situ laboratory study on influencing factors of pre-SC-CO_2 hybrid fracturing effect in shale oil reservoirs. Petrol. Sci. https://doi.org/10.1016/j.petsci.2024.05.020.
Zeng, L.P., Lu, Y.H., Al Maskari, N.S., et al., 2020. Interpreting micromechanics of fluid-shale interactions with geochemical modelling and disjoining pressure: implications for calcite-rich and quartz-rich shales. J. Mol. Liq. 319. https://doi.org/10.1016/j.molliq.2020.114117.
Zhang, C.P., Liu, S., Ma, Z.Y., et al., 2021. Combined micro-proppant and supercritical carbon dioxide (SC-CO_2) fracturing in shale gas reservoirs: a review. Fuel 305. https://doi.org/10.1016/j.fuel.2021.121431.
Zhang, F.S., An, M.K., Zhang, L.Y., et al., 2020. Effect of mineralogy on friction-dilation relationships for simulated faults: implications for permeability evolution in caprock faults. Geosci. Front. 11 (2), 439–450. https://doi.org/10.1016/j.gsf.2019.05.014.
Zhang, F.S., Shen, Y.D., Wang, X.R., et al., 2013. Synthesis and propertis of sulfonate surfactant fracturing fluid. Oilfield Chem. 30 (2), 179–183. https://doi.org/10.19346/j.cnki.1000-4092.2013.02.005 (in Chinese).
Zhang, J., Li, X.X., Li, Y.W., et al., 2021. Experimental research and numerical simulation: strength and rupture patterns of coal under Brazilian tensile test. Int. J. Oil Gas Coal Technol. 26 (2), 225–244. https://doi.org/10.1504/ijogct2021.10035079.
Zhang, J., Li, Y.W., Pan, Y.S., et al., 2021. Experiments and analysis on the influence of multiple closed cemented natural fractures on hydraulic fracture propagation in a tight sandstone reservoir. Eng. Geol. 281, 105981. https://doi.org/10.1016/j.enggeo.2020.105981.
Zhang, N.L., Luo, Z.F., Zhao, L.Q., et al., 2022. Innovative thermo-responsive in-situ generated proppant: laboratory tests and field application. J. Petrol. Sci. Eng. 208. https://doi.org/10.1016/j.petrol.2021.109514.
Zhang, W., Wang, C.G., Guo, T.K., et al., 2021. Study on the cracking mechanism of hydraulic and supercritical CO_2 fracturing in hot dry rock under thermal stress. Energy 221. https://doi.org/10.1016/j.energy.2021.119886.
Zhang, W., Wang, Q., 2018. Permeability anisotropy and gas slippage of shales from the Sichuan Basin in South China. Int. J. Coal Geol. 194, 22–32. https://doi.org/10.1016/j.coal.2018.05.004.
Zhang, X.W., Lu, Y.Y., Tang, J.R., et al., 2017. Experimental study on fracture initiation and propagation in shale using supercritical carbon dioxide fracturing. Fuel 190, 370–378. https://doi.org/10.1016/j.fuel.2016.10.120.
Zhang, X.X., Wang, J.G., Gao, F., et al., 2017. Impact of water, nitrogen and CO_2 fracturing fluids on fracturing initiation pressure and flow pattern in anisotropic shale reservoirs. J. Nat. Gas Sci. Eng. 45, 291–306. https://doi.org/10.1016/j.jngse.2017.06.002.
Zhang, Y.X., He, J.M., Li, X., et al., 2019. Experimental study on the supercritical CO_2 fracturing of shale considering anisotropic effects. J. Petrol. Sci. Eng. 173, 932–940. https://doi.org/10.1016/j.petrol.2018.10.092.
Zhang, Z.B., Li, X., 2016. Numerical study on the formation of shear fracture network. Energies 9 (4), 299. https://doi.org/10.3390/en9040299.
Zhao, H.Q., Wu, K., Huang, Z.W., et al., 2021. Numerical model of CO_2 fracturing in naturally fractured reservoirs. Eng. Fract. Mech. 244. https://doi.org/10.1016/j.engfraemech.2021.107548.
Zhao, J., Fan, J., Mao, J., et al., 2018. High performance clean fracturing fluid using a new tri-cationic surfactant. Polymers 10 (5), 535. https://doi.org/10.3390/polym10050535.
Zhao, J.Z., Chen, P.F., Liu, Y.Q., et al., 2018. Development of an LPG fracturing fluid with improved temperature stability. J. Petrol. Sci. Eng. 162 (0920–4105), 548–553. https://doi.org/10.1016/j.petrol.2017.10.060.
Zhao, Y., Yu, Q.C., 2017. CO_2 breakthrough pressure and permeability for unsaturated low-permeability sandstone of the Ordos Basin. J. Hydrol. 550, 331–342. https://doi.org/10.1016/j.jhydrol.2017.04.050.
Zheng, Y., Wang, H.Z., Li, G.S., et al., 2022a. Proppant transport characteristics in tortuous fractures induced by supercritical CO_2 fracturing. Nat. Gas. Ind. B 9 (5), 457–466. https://doi.org/10.1016/j.ngib.2022.03.005.
Zheng, Y., Wang, H.Z., Li, Y.J., et al., 2022b. Effect of proppant pumping schedule on the proppant placement for supercritical CO_2 fracturing. Petrol. Sci. 19 (2), 629–638. https://doi.org/10.1016/j.petsci.2021.11.002.
Zheng, Y., Wang, H.Z., Tian, G.H., et al., 2022c. Experimental investigation of proppant transport in hydraulically fractured wells using supercritical CO_2. J. Petrol. Sci. Eng. 217 (15), 110907. https://doi.org/10.1016/j.petrol.2022.110907.
Zheng, Y., Wang, H.Z., Yang, B., et al., 2020. CFD-DEM simulation of proppant transport by supercritical CO_2 in a vertical planar fracture. J. Nat. Gas Sci. Eng. 84, 103647. https://doi.org/10.1016/j.jngse.2020.103647.
Zheng, Y., Zhou, M.M., Kuru, E., et al., 2024. Proppant transport in rough fracture networks using supercritical CO_2. Petrol. Sci. 21 (3), 1852–1864. https://doi.org/10.1016/j.petsci.2024.03.023.
Zhou, D.W., Zhang, G.Q., Prasad, M., et al., 2019. The effects of temperature on supercritical CO_2 induced fracture: an experimental study. Fuel 247, 126–134. https://doi.org/10.1016/j.fuel.2019.02.099.
Zhou, J., Yang, K., Tian, S., et al., 2020. CO_2-water-shale interaction induced shale microstructural alteration. Fuel 263, 116642. https://doi.org/10.1016/j.fuel.2019.116642.
Zhou, J.P., Hu, N., Xian, X.F., et al., 2019. Supercritical CO_2 fracking for enhanced shale gas recovery and CO_2 sequestration: results, status and future challenges. Adv. Geo-Energy Res. 3 (2), 207–224. https://doi.org/10.26804/ager.2019.02.10.
Zhou, J.P., Kuang, N.J., Tian, S.F., et al., 2022. Status quo of water-free fracturing technology for shale gas reservoirs. Natural Gas Tech. Econ. 16 (6), 49–55. https://doi.org/10.3969/j.issn.2095-1132.2022.06.008 (in Chinese).
Zhou, M., Ni, R., Zhao, Y., et al., 2021. Research progress on supercritical CO_2 thickeners. Soft Matter 17 (20), 5107–5115. https://doi.org/10.1039/d1sm00189b.
Zhou, W., Shi, G.X., Wang, J.B., et al., 2022. The influence of bedding planes on tensile fracture propagation in shale and tight sandstone. Rock Mech. Rock Eng. 55 (3), 1111–1124. https://doi.org/10.1007/s00603-021-02742-2.
Zhou, X., Burbey, T.J., 2013. Fluid effect on hydraulic fracture propagation behavior: a comparison between water and supercritical CO_2-like fluid. Geofluids 14 (2), 174–188. https://doi.org/10.1111/gfl.12061.
Zhou, Y., Ni, H.J., Shen, Z.H., et al., 2020. Numerical simulation of temperature field in crack of supercritical carbon dioxide fracturing. Energy Sci. Eng. 8 (6), 2141–2150. https://doi.org/10.1002/ese3.653.
Zhu, K., Zhong, D.W., Zhou, G.S., 2022. Performance research and application of carbon dioxide expansion blasting one-time cracking pipe. Blasting 39 (2), 133–139. https://doi.org/10.3969/j.issn.1001-487x.2022.02.020.
Zhuang, Z.J., Li, M., Zhang, L.Q., et al., 2023. Summary of physical parameters of supercritical carbon dioxide. Low Temp. Special. Gas. 41 (5), 8–15+20. https://doi.org/10.3969/j.issn.1007-7804.2023.05.002 (in Chinese).
Zou, Y.S., Li, N., Ma, X.F., et al., 2018a. Experimental study on the growth behavior of supercritical CO_2-induced fractures in a layered tight sandstone formation. J. Nat. Gas Sci. Eng. 49, 145–156. https://doi.org/10.1016/j.jngse.2017.11.005.
Zou, Y.S., Li, S.H., Ma, X.F., et al., 2018b. Effects of CO_2–brine–rock interaction on porosity/permeability and mechanical properties during supercritical-CO_2 fracturing in shale reservoirs. J. Nat. Gas Sci. Eng. 49, 157–168. https://doi.org/10.1016/j.jngse.2017.11.004.
Zuo, L., Han, H.M., Jiang, T.X., et al., 2021. Research on Fracture propagation mechanism and technology of carbon dioxide fracturing in shale gas. Drilling and Production Technology, 44 (5), 45–49. https://doi.org/10.3969/j.issn.1006.768x.2021.05.10 (in Chinese).